AGU ADVANCING EARTH AND SPACE SCIENCES

AGU Advances

RESEARCH ARTICLE
10.1029/2023AV001000

Distribution and Drivers of Organic Carbon Sedimentation Along the Continental Margins

Logan A. Tegler[1,2,3,4], Tristan J. Horner[1,2], Valier Galy[2], Shavonna M. Bent[2,3], Yi Wang[1,5], Heather H. Kim[2], Öykü Z. Mete[6], and Sune G. Nielsen[1,7]

[1]NIRVANA Laboratories, Woods Hole Oceanographic Institution, Woods Hole, MA, USA, [2]Department of Marine Chemistry and Geochemistry, Woods Hole Oceanographic Institution, Woods Hole, MA, USA, [3]Department of Earth, Atmospheric and Planetary Sciences, Massachusetts Institute of Technology, Cambridge, MA, USA, [4]Now at Department of Oceanography, School of Ocean and Earth Science and Technology, University of Hawa'i at Mānoa, Honolulu, HI, USA, [5]Now at Department of Earth and Environmental Sciences, Tulane University, New Orleans, LA, USA, [6]Department of Earth and Planetary Sciences, Harvard University, Cambridge, MA, USA, [7]Now at CRPG, CNRS, Université de Lorraine, Metz, France

Peer Review The peer review history for this article is available as a PDF in the Supporting Information.

Key Points:

- Between 17.4 and 24.5 Tmol (0.2–0.3 Pg) of organic carbon (OC) are sedimented on the seafloor annually, of which 90% is along continental margins
- More than 95% of marine OC sedimentation occurs in regions with bottom-water oxygen concentrations >50 μmol kg^{-1}
- The ability to escape remineralization, rather than production at the sea surface, sets the global pattern of OC sedimentation

Supporting Information:

Supporting Information may be found in the online version of this article.

Correspondence to:

L. A. Tegler and T. J. Horner,
tegler@hawaii.edu;
tristan.horner@whoi.edu

Citation:

Tegler, L. A., Horner, T. J., Galy, V., Bent, S. M., Wang, Y., Kim, H. H., et al. (2024). Distribution and drivers of organic carbon sedimentation along the continental margins. *AGU Advances*, *5*, e2023AV001000. https://doi.org/10.1029/2023AV001000

Received 25 JUL 2023
Accepted 18 JUL 2024

Author Contributions:

Conceptualization: Logan A. Tegler, Tristan J. Horner, Valier Galy, Shavonna M. Bent, Sune G. Nielsen
Data curation: Logan A. Tegler, Heather H. Kim
Formal analysis: Logan A. Tegler, Öykü Z. Mete
Funding acquisition: Logan A. Tegler, Tristan J. Horner, Sune G. Nielsen

Abstract Organic carbon (OC) sedimentation in marine sediments is the largest long-term sink of atmospheric CO_2 after silicate weathering. Understanding the mechanistic and quantitative aspects of OC delivery and preservation in marine sediments is critical for predicting the role of the oceans in modulating global climate. Yet, estimates of the global OC sedimentation in marginal settings span an order of magnitude, and the primary controls of OC preservation remain highly debated. Here, we provide the first global bottom-up estimate of OC sedimentation along the margins using a synthesis of literature data. We quantify both terrestrial- and marine-sourced OC fluxes and perform a statistical analysis to discern the key factors influencing their magnitude. We find that the margins host 23.2 ± 3.5 Tmol of OC sedimentation annually, with approximately 84% of marine origin. Accordingly, we calculate that only 2%–3% of OC exported from the euphotic zone escapes remineralization before sedimentation. Surprisingly, over half of all global OC sedimentation occurs below bottom waters with oxygen concentrations greater than 180 μM, while less than 4% occurs in settings with <50 μM oxygen. This challenges the prevailing paradigm that bottom-water oxygen (BWO) is the primary control on OC preservation. Instead, our statistical analysis reveals that water depth is the most significant predictor of OC sedimentation, surpassing all other factors investigated, including BWO levels and sea-surface chlorophyll concentrations. This finding suggests that the primary control on OC sedimentation is not production, but the ability of OC to resist remineralization during transit through the water column and while settling on the seafloor.

Plain Language Summary Particulate organic carbon (OC) sedimentation is a major sink of atmospheric carbon dioxide. Most OC is thought to be sedimented along the margin, the marine area near land with water depths shallower than 1,500 m. However, estimating how much OC is sedimented in these environments has proven challenging with current methods. Here, we compiled and studied information on hundreds of seafloor sediment samples that were collected from around the world. We find that the margins account for approximately 92% of total marine OC sedimentation. Surprisingly, less than 4% of this sedimentation occurs in low-oxygen regions of the ocean, contradicting a long-standing assumption about the importance of low-oxygen regions to global carbon sedimentation. Our results show that the breakdown of particulate OC during its transit through the water column and while settling at the seafloor is the main control on how much OC is sedimented. This information helps to constrain the flux of several other biologically cycled elements and will be important for predicting how global climate change will affect marine OC sedimentation.

1. Introduction

Nearly 40% of global net primary production (NPP) occurs in the ocean, equivalent to the production of about 6,500 Tmol organic carbon (OC) $year^{-1}$ (Falkowski et al., 1998; Jin et al., 2006). Around 850 Tmol (~15%) of this OC is exported below the euphotic zone and an additional ~37.5 Tmol of terrestrial OC is delivered from continental environments via rivers (Galy et al., 2015; Hedges et al., 1997). Though much of this OC is remineralized before it reaches the seafloor (Dunne et al., 2007; Jahnke, 1996; Martin et al., 1987), OC burial is

Investigation: Logan A. Tegler, Tristan J. Horner, Valier Galy, Heather H. Kim, Öykü Z. Mete, Sune G. Nielsen
Methodology: Logan A. Tegler, Tristan J. Horner, Valier Galy, Shavonna M. Bent, Yi Wang, Heather H. Kim, Öykü Z. Mete, Sune G. Nielsen
Resources: Logan A. Tegler, Heather H. Kim
Software: Logan A. Tegler, Tristan J. Horner, Heather H. Kim, Öykü Z. Mete, Sune G. Nielsen
Supervision: Tristan J. Horner, Sune G. Nielsen
Validation: Logan A. Tegler, Öykü Z. Mete
Visualization: Logan A. Tegler, Tristan J. Horner, Öykü Z. Mete, Sune G. Nielsen
Writing – original draft: Logan A. Tegler, Tristan J. Horner, Sune G. Nielsen
Writing – review & editing: Logan A. Tegler, Tristan J. Horner, Valier Galy, Shavonna M. Bent, Yi Wang, Heather H. Kim, Öykü Z. Mete, Sune G. Nielsen

one of the two major long-term sinks of atmospheric carbon dioxide (CO_2), the other being silicate weathering (Urey, 1952).

Despite its importance to the C cycle, the very definition of OC burial is murky, which makes estimating fluxes challenging. True burial refers to OC irreversibly stored in sediments below the active degradation zone (Keil, 2015). Ideally, we want to quantify this flux of OC because it is removed from the surficial C cycle on tectonic timescales (Walker, 1993). However, determining this depth is difficult, as the depth at which OC remineralization is arrested is highly variable, and may not even exist (Bradley et al., 2022). Moreover, when constructing a burial estimate using literature data without sediment or pore water information to assess OC degradation in the sediment, it is impossible to ensure that every datum is below the zone of active degradation. Given these limitations, we focus our study on *OC sedimentation*, which we define as a flux that falls between the OC rain rate and the OC flux at the depth of irreversible burial. Thus, any sediment-based estimate of global OC sedimentation is likely to represent an upper bound of the true OC burial flux.

In addition to the challenge of defining burial, studies have shown that determining the magnitude and spatial pattern of OC sedimentation is also difficult, especially along the continental margins, where most OC sedimentation is thought to occur (Bianchi et al., 2018; Burdige, 2007). In contrast, deep-sea OC sedimentation (i.e., below 1,500 m, or ∼85% of the ocean floor) is more easily quantified, but constitutes a small flux relative to that sedimented in marginal settings (Hayes et al., 2021). The sedimentation of OC is much larger in margin sediments than in deep-sea sediments for two principle reasons: productivity and proximity. Marginal environments are, by definition, closer to the land, which can provide essential nutrients that can stimulate plankton growth (e.g., from coastal upwelling, terrestrial run-off, and sediment dissolution). Likewise, margin environments are shallower than the deep sea, meaning that there is a shorter distance for OC to travel between where it is produced and where it is sedimented. Despite their importance to the global C budget, OC fluxes to the margins are not well constrained (Table 1). The lack of constraints reflects, in significant part, the sparsity of measurements in margin environments relative to their high degree of heterogeneity. While it is possible to measure the flux of OC accumulating in any individual sediment sample, OC fluxes can vary greatly over relatively small distances due to variations in seafloor topography, water column oxygen concentrations, rates of nutrient-rich water mass upwelling, and ecological factors that affect export and remineralization (Arndt et al., 2013; Bauer et al., 2013; Eglinton et al., 2021; Hedges & Keil, 1995; Middelburg, 2018). While previous studies have been able to derive estimates of margin OC fluxes using global sediment averages (Gershanovich et al., 1974), such estimates cannot account for regional variations in OC fluxes. Quantifying and understanding the spatial pattern of OC sedimentation in margin sediments therefore requires alternative approaches that can account for regional heterogeneity.

Almost all published estimates of margin OC sedimentation are based on "top-down" approaches. Top-down approaches are popular because they offer granular information on OC sedimentation, which is necessary to account for regional heterogeneity. Top-down models achieve this by using input data with a high spatial sampling density, such as sea-surface chlorophyll concentrations or temperature, which can be determined via satellite. Global OC sedimentation can then be modeled by considering how much OC is produced (i.e., NPP), the fraction of the produced OC that is exported out of the euphotic zone, how much is transferred through the water column, and the amount of OC that is expected to arrive at the seafloor. These latter terms have been estimated using combinations of sediment trap data and benthic O_2 fluxes (e.g., Jahnke, 2010) or through empirical relationships derived from data sets of water column particulate OC fluxes and sedimentation rates (e.g., Dunne et al., 2005, 2007; Lutz et al., 2002). While valuable, these approaches require explicit parameterizations of processes that may be poorly understood mechanistically, leading to global margin OC sedimentation flux estimates varying by almost a factor of 40 (Table 1).

The wide range of top-down OC sedimentation estimates suggests that bottom-up approaches—those that leverage measurements of the sediments themselves—may also be valuable in constraining global OC fluxes. However, bottom-up approaches for measuring OC fluxes present several of their own challenges, such as: sparse input data, the need to differentiate between types of OC, and the very definition of burial and sedimentation. In general, there are far fewer measurements of OC fluxes than OC concentrations. Several studies employed machine-learning and other statistical approaches to estimate sedimentary OC stocks (Atwood et al., 2020; Lee et al., 2019), but not OC fluxes. Where bottom-up estimates of OC fluxes do exist, these studies typically focus on specific regions with high data density, rather than extrapolating to all margins (Diesing et al., 2021; Smeaton

Table 1
A Compliation of Existing Marine Organic Carbon Sedimentation Flux Estimates

Marine OC sedimentation rate (Tg C year^{-1})	Marine OC sedimentation rate (Tmol C year^{-1})	Reference	Estimate logic
60	5	Muller-Karger et al. (2005)	Used satellite data and NPP estimates. The NPP estimates were attenuated with depth to the seafloor using standard models
2,218	184.7	Archer et al. (2002)	Diagenesis model was applied to a gridded map of OC rain rates across bottom water oxygen value
590	49.2	Middelburg et al. (1997)	Used empirical relationships between remineralization rates and water depth (geometric mean was taken)
2,481	206.6	Middelburg et al. (1997)	Used empirical relationships between remineralization rates and water depth combined with arithmetic means (arithmetic mean)
213	17.7	Muller-Karger et al. (2005) Burdige (2007)	The OC rain rate from this work was assumed to be the rate of marine organic matter input to sediments, and sedimentation efficiency values taken from another study (Burdige, 2007; Muller-Karger et al., 2005). These were applied to these rain rates to estimate sedimentation rates of marine organic carbon
577	48	Burdige (2007)	Estimated sedimentation efficiency based on remineralization rates. Study assumed a steady-state OC budget
248	20.6	Burdige (2007)	Same as above method, but estimate assumed relict sands do not accumulate very much TOC
149	12.1	Hedges and Keil (1995)	Estimate was recalculated from another reference (Berner, 1989)
218	18.2	Gershanovich et al. (1974)	Average TOC content of Holocene sediments multiplied by their areal size and thickness
187.08	15.6	Jahnke (2010)	Regionally defined fluxes from oxygen fluxes and primary productivity
290.4	24.2	Dunne et al. (2007)	Series of algorithms starting with satellite estimate of primary productivity, converted to a sinking particle flux, estimated penetration to the sea floor, and finally accumulation in the sediments
231.6	19.4	This study	Interpolation and extrapolation of patterns of OC sedimentation

et al., 2021). Another difficulty concerns the different types of OC present in marine sediments. Marine sedimentary OC often contains a mixture of autochthonous (produced in the ocean) and allochthonous OC (formed in the terrestrial environment and transported to the seafloor). This mixing of OC types necessitates that OC from terrestrial and marine environments be tabulated separately if we aim to constrain the magnitude and efficiency of the marine biological carbon pump and exclude terrestrial inputs.

Here, we estimate margin OC sedimentation using a bottom-up, data-driven approach leveraging more than 800 OC sedimentation rates from recent environments (i.e., Holocene; younger than 11,000 years before the present) deposited in water depths shallower than 1,500 m. Our estimate accounts for vertical and spatial variability in OC sedimentation along continental margins by employing geospatial interpolation methods, allowing us to arrive at an annual global margin OC sedimentation estimate. Combining this flux with an existing bottom-up estimate of deep-sea OC sedimentation fluxes from Hayes et al. (2021), we calculate global OC sedimentation. To interrogate the controls on this flux estimate, we employ multiple linear regression (MLR) modeling using standard oceanographic predictors. Our marine flux offers a new means to calculate the efficiency of the biological carbon pump and has implications for the sedimentation of other biologically cycled elements.

2. Materials and Methods

Our methodology for estimating OC sedimentation involved five main steps: data compilation, categorizing based on OC type and water depth (Section 2.1), interpolation, extrapolation for regional coverage, and region-specific analysis (Section 2.2). Following these steps, we employed MLR analysis to study the predictability of OC sedimentation and identify the main features that control it (Section 2.3).

2.1. Data Compilation and Categorization

Organic carbon sedimentation data were compiled from the PANGAEA database (pangaea.de), Integrated Ocean Discovery Program (IODP) proceedings (publications.iodp.org), and through literature searches (Table S1 in Supporting Information S3). Many of the compiled data possessed a mass accumulation rate (MAR); however, for samples without an associated MAR, we assumed a linear sedimentation rate between sediment samples in cores that had age and depth constraints and multiplied by the dry bulk density:

$$\text{MAR} = \text{Sedimentation Rate}\left(\text{cm year}^{-1}\right) \times \text{dry bulk density}\left(\frac{\text{g}}{\text{cm}^3}\right) \quad (1)$$

This process resulted in a MAR for every sample. The rate of OC sedimentation was obtained by multiplying the MAR by the OC content of each sample:

$$\text{OC}_{\text{sedimentation}} = \text{MAR}\left(\text{g cm}^{-2}\ \text{year}^{-1}\right) \times \frac{\text{OC (wt.\%)}}{100} \quad (2)$$

While total OC sedimentation data are useful, they combine autochthonous and allochthonous OC. Since only the former is useful for assessing marine CO_2 removal, we split the data into two data sets to isolate samples that may have significant terrestrial OC influence. The first data set included sediment samples with both marine and terrestrial influence (Figure 1a; $n = 804$), whereas samples that were strongly influenced by terrestrially sourced OC were removed from the second data set (Figure 1b; "predominantly marine" $n = 691$). The terrestrial influence was assessed based on C:N ratios and $\delta^{13}C$ values. In general, terrestrial OC exhibits C:N > 10 (Lamb et al., 2006), whereas most marine OC exhibits C:N between 5 and 8 (Redfield, 1934). Likewise, the $\delta^{13}C$ of terrestrial OC is typically between −21 and −32‰, which is lower than the majority of marine OC (−18 to −24‰; Lamb et al., 2006). As such, terrestrial organic matter was screened from the predominantly marine data set by removing samples with C:N > 8 or $\delta^{13}C < -23$‰. Although this screening does not eliminate all terrestrial organic matter influence, particularly if the terrestrial OC is dominated by C_4 plants (Lamb et al., 2006), samples falling outside both the terrestrial screening values (C:N < 8 and $\delta^{13}C > -23$‰) in marine sediments likely have relatively minor terrestrial components. Samples previously used in marine estimates were retained in the marine compilation regardless of whether they had published C:N or $\delta^{13}C$ values (Cartapanis et al., 2016; Hayes et al., 2021). This method, while potentially allowing some terrestrial influence, prioritizes having more data with minimal terrestrial material than having fewer data, which should provide a more robust estimate of marine OC sedimentation.

2.2. Interpolation and Extrapolation of OC Sedimentation Estimates

Following initial data compilation, a map of seafloor topography (Smith & Sandwell, 1997) was loaded into ArcMap (Version 10.8.2; Esri, Redlands CA) and projected so that each pixel had an equal area (1 km^2 pixel size; Figure 1a). The distinction between the continental margins and the deep sea was challenging to define due to the unique hydrography of each region. Previous studies have placed the boundary between the margins and the deep sea between 1,000 and 2,000 m (Burdige, 2007; Hayes et al., 2021). For this study, we defined the margin as encompassing depths ranging from 0 to 1,500 m, including the continental shelf (0–200 m; Laruelle et al., 2013). Deeper depths were excluded as robust OC flux estimates for the deep ocean are available in Hayes et al. (2021), and because the deep-sea OC flux is relatively small compared to that of the margins.

Subsequently, we created two bathymetry bins (0–1,000 m and 1,000–1,500 m water depth), and the compiled OC sedimentation data were loaded into ArcMap. Within each bin, the data were interpolated and extrapolated using inverse distance weighting (IDW). This deterministic interpolation technique estimates values at unsampled locations based on the values at the nearest sampled locations according to a distance decay function. The closer an unsampled point is to an observation, the more weight that point has in the averaging process. The significance that the nearest point has relative to further ones is controlled by defining the "power." A higher power places an additional emphasis on the nearest points, whereas a lower power places less emphasis on these points. We used a power of two (i.e., 1/distance^2), meaning that a sample twice as far away from the target pixel as another sample would be weighted four times less.

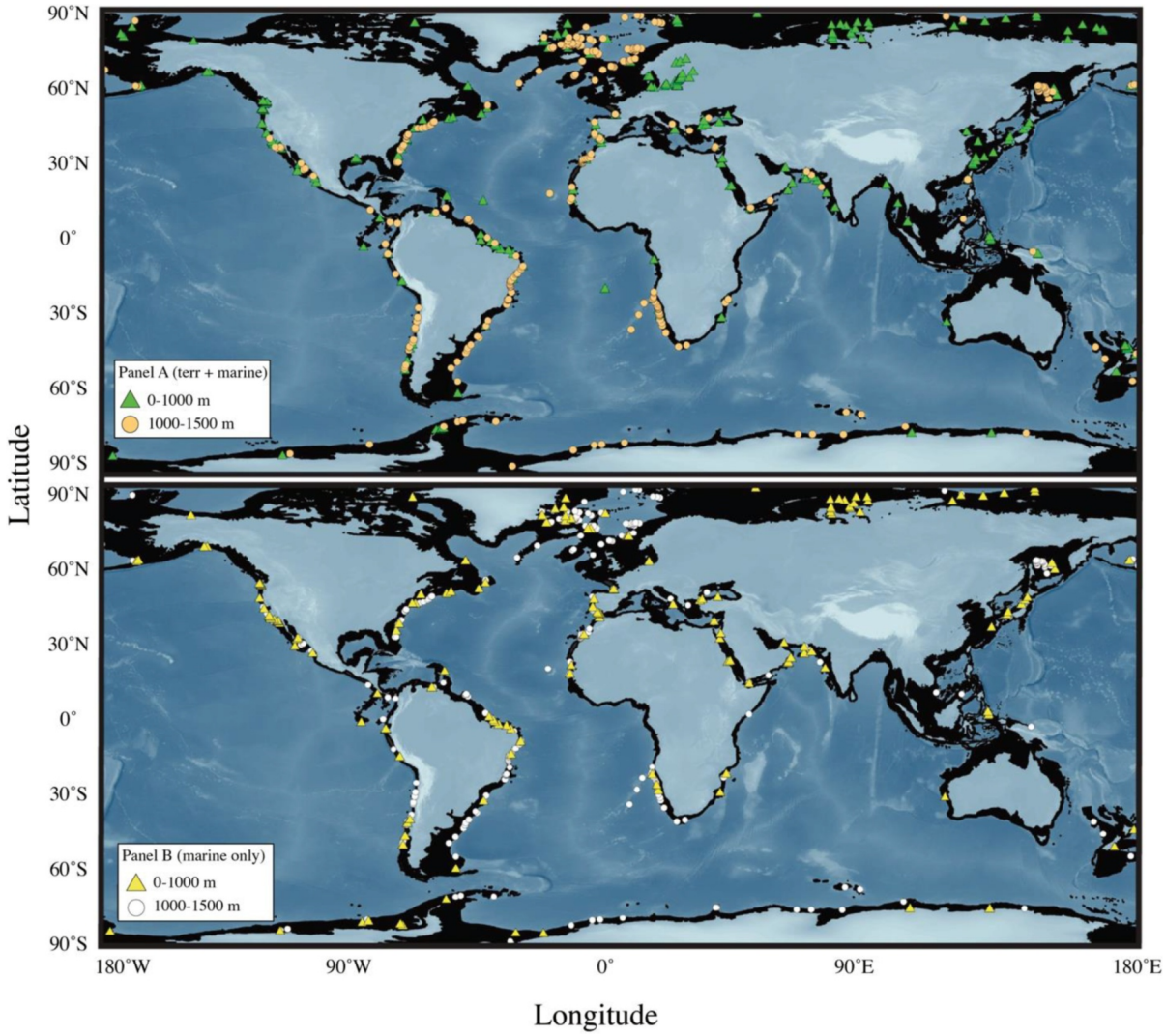

Figure 1. Global map of compiled sediments with organic carbon (OC) sedimentation. Black regions show continental margins with bathymetry <1,500 m. (a) Shows samples that include both terrestrial and marine OC sedimentation. The triangles are data between 0 and 1,000 m and the circles are data between 1,000 and 1,500 m. (b) Includes only sediments with marine-dominated OC. The triangles are data from 0 to 1,000 m and the circles are data from 1,000 to 1,500 m.

By default, ArcMap interpolates over the data within a minimum spatial bounding box that encompasses all the data. However, this does not allow ArcMap to produce a map that covers the entire region of interest. Thus, we created a bounding box using extrapolation that was larger than the minimum spatial bounding box and covered the entire region. To do this, the processing extent box was set to the size of each region of interest (Figure 2, Table 2). Extrapolated OC fluxes were bounded by the values encountered in that region; extrapolations could not yield OC sedimentation rates that were more (or less) than the largest (or smallest) observed OC sedimentation rate within the bounding box. Once every pixel had a defined flux, the pixels were summed to produce a total OC sedimentation for the defined area.

The spatial binning reveals sampling biases. Some regions are data-dense and are presumed to give the most accurate interpolations. Conversely, some areas have too little data to interpolate. Therefore, we divided the margin into 30 distinct regions, which constrained the distance over which any individual datum can be interpolated within that region. For each region, we assessed if alternative methods were required to obtain the most robust OC sedimentation flux. These methods either used the higher-density data within one bathymetric bin to extrapolate a flux to the other bin or, in a few cases with particularly poor data coverage, adopted previous

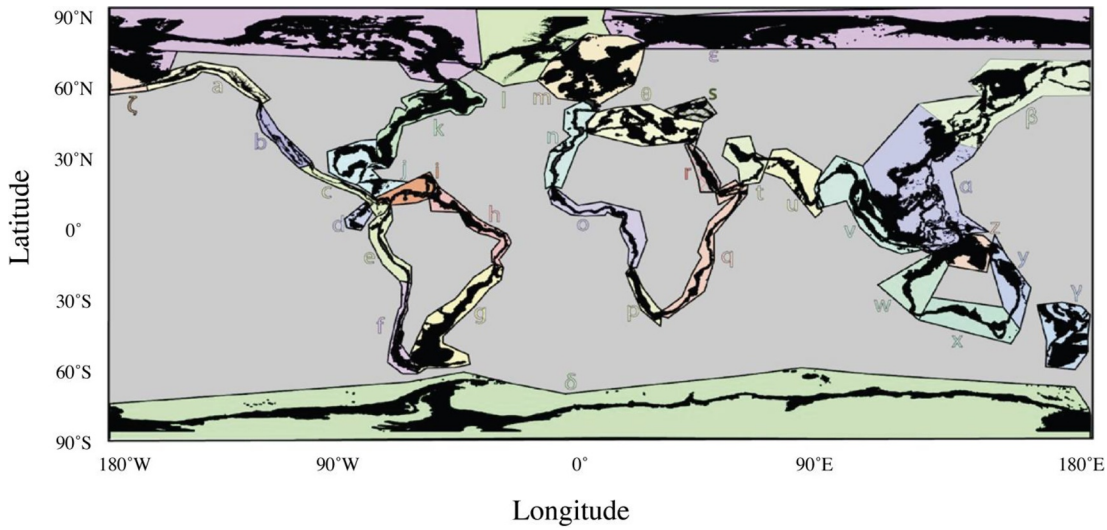

Figure 2. Map showing the 30 regions (each labeled with a letter) we divided the margin in. The black area is the seafloor from 0 to 1,500 m water depth. The colored part around each region illustrates where the boundaries of the regions are. Each region is given a letter so that it can be referred to more easily without depending on the names of landmass (Table 2).

estimates from the literature. These details are included in the results and discussion. A complete ArcMap workflow can be found within Supporting Information S1.

2.3. Constructing Multiple Linear Regression Models

To augment our IDW-based estimates of marine OC sedimentation, we employed statistical modeling of OC flux data using MLR without interaction terms. This approach had two main objectives: to assess the predictability of OC fluxes based on a set of features and to identify the features that exert the most significant influence on predicting OC fluxes.

The MLR analysis incorporated 12 predictor values derived from two databases: World Ocean Atlas 2018 (WOA18) and Copernicus Marine Service (CMEMS) satellite data. The WOA18 provided mixed layer depth (MLD), surface- and bottom-water temperature (BWT), and dissolved oxygen, as well as sea-surface nutrients (nitrate, phosphate, and silicate), while CMEMS data contributed surface chlorophyll-a levels. Nearest-neighbor interpolation was then used to infer values for the location of each of the OC flux values in our sediment compilation. For all data extracted from the WOA18, objectively analyzed mean data were obtained from the 1° grid at the depth level corresponding to the sediment sample. For the CMEMS satellite data, surface chlorophyll-a values were interpolated onto a 4-km grid. This process resulted in a data set containing 459 observations of OC fluxes associated with all 12 predictor variables. Approximately 200 data points were excluded because one or more predictor variables could not be located for the latitude and longitude of the OC flux datum. The OC sedimentation and chlorophyll-a data were then log transformed to reduce parameter weighting and MLR models were employed to predict OC fluxes using the MATLAB *fitlm* function. The general form of the MLR equation is as follows:

$$\mathrm{OC}_{\mathrm{sedimentation}} = c + \beta_1 \cdot \mathrm{longitude} + \beta_2 \cdot \mathrm{latitude} + \beta_3 \cdot \mathrm{depth} + \beta_4 \cdot \mathrm{SWT} + \beta_5 \cdot \mathrm{BWT} +$$

$$\beta_6 \cdot \mathrm{BWO} + \beta_7 \cdot \mathrm{SWO} + \beta_8 \cdot \mathrm{SWSi} + \beta_9 \cdot \mathrm{SWP} + \beta_{10} \cdot \mathrm{SWN} + \beta_{11} \cdot \mathrm{Chl} + \beta_{12} \cdot \mathrm{MLD}$$

where c is the intercept and β_n represents the optimized coefficient for each of the 12 predictors: longitude, latitude, depth, surface-water temperature (SWT), BWT, bottom-water oxygen (BWO), surface-water oxygen (SWO), surface water silicate (SWSi), surface-water phosphate (SWP), surface-water nitrate (SWN), chlorophyll-a levels (Chl), and MLD. Following Mete et al. (2023), we used a factorial design to test 4,095 distinct MLR models. In this framework, each model represented a unique combination of the 12 features, which were either enabled (and optimized) or disabled (set to zero). This design theoretically allowed for 2^{12} (4,096)

Table 2
Combined Marine and Terrestrial Organic Carbon (OC) Fluxes

General region	Figure code	Area in km^2 (0–1,000 m)	Area in km^2 (1,000–1,500 m)	Total area (km^2)	OC flux (mol m^{-2} year^{-1})	OC flux (Tmol year^{-1})	Source
Northeast Pacific	a	5.74E+05	3.08E+04	6.05E+05	2.09	1.26	This study
Northeast Pacific	b	3.32E+05	6.96E+04	4.02E+05	2.04	0.86	This study
Northeast Pacific	c	2.16E+05	5.28E+04	2.69E+05	0.65	0.18	This study
Equatorial Pacific	d	3.43E+04	4.53E+04	7.96E+04	0.25	0.02	This study
Southeast Pacific	e	2.27E+05	6.63E+04	2.93E+05	0.86	0.25	This study
Southeast Pacific	f	2.66E+05	3.37E+04	3.00E+05	0.76	0.23	This study
Southwest Atlantic	g	1.79E+06	1.69E+05	1.96E+06	0.12	0.23	This study
Southwest Atlantic	h	6.50E+05	8.43E+04	7.34E+05	1.91	1.4	This study
West Equatorial Atlantic	i	2.94E+05	1.01E+05	3.95E+05	0.75	0.37	This study
Gulf of Mexico	j	1.02E+06	2.17E+05	1.24E+06	0.17	0.21	This study
Northwest Atlantic	k	1.79E+06	1.21E+05	1.91E+06	0.05	0.1	This study
Arctic	l	7.48E+05	2.36E+05	9.84E+05	0.62	0.61	This study
Northeast Atlantic	m	1.81E+06	3.52E+05	2.16E+06	0.55	1.2	This study
Northeast Atlantic	n	4.23E+05	8.50E+04	5.08E+05	0.72	0.37	This study
Southeast Atlantic	o	4.83E+05	9.44E+04	5.77E+05	0.21	0.12	This study
Southeast Atlantic	p	3.98E+05	5.98E+04	4.58E+05	0.16	0.07	This study
West Indian	q	4.82E+05	1.75E+05	6.57E+05	0.19	0.12	This study
Red Sea	r	3.99E+05	5.59E+04	4.55E+05	0.02	0.01	This study
Black Sea	s	2.08E+05	3.39E+04	2.42E+05	0.2	0.05	This study
West Arabian Sea	t	3.61E+05	2.65E+04	3.88E+05	0.46	0.18	This study
East Arabian Sea	u	4.47E+05	7.36E+04	5.21E+05	0.16	0.08	This study
Bay of Bengal	v	1.29E+06	2.31E+05	1.52E+06	0.59	0.90	This study
Australia (West)	w	5.81E+05	1.79E+05	7.60E+05	0.12	0.09	Jahnke
Australia (South)	x	5.75E+05	5.69E+04	6.32E+05	0.21	0.13	Jahnke
Australia (East)	y	7.20E+05	1.40E+05	8.60E+05	0.23	0.20	Jahnke (2010)
Australia (Tropical)	z	1.33E+06	2.49E+04	1.35E+06	0.25	0.34	Jahnke (2010)
West Equatorial Pacific	α	4.50E+06	5.07E+05	5.01E+06	1.05	5.24	This study
Northwest Pacific	β	2.03E+06	4.83E+05	2.51E+06	0.16	0.39	This study
Antarctic	δ	1.03E+06	5.81E+05	1.61E+06	0.54	2.35	This study
South Pacific	ɣ	4.03E+06	3.40E+05	4.37E+06	0.22	0.36	This study
Arctic	ε	8.11E+06	2.98E+05	8.41E+06	0.62	5.21	This study
Northeast Pacific	ζ	2.65E+04	2.78E+04	5.43E+04	0.06	0.02	This study
Mediterranean Sea	ϑ	1.07E+06	2.27E+05	1.30E+06	0.02	0.03	This study
Sum		3.82E+07	5.3E+06	4.35E+07		23.2	

possible feature combinations; however, due to the necessity of having at least one feature enabled per model, the total count of unique, trainable MLR models with ≥1 features = $2^{12} - 1 = 4{,}095$.

We used Monte Carlo cross-validation to assess MLR model performance. Specifically, before MLR model initialization and optimization, the data set was randomly partitioned into training (75%) and validation (25%) components. The training component was used to compute the best fit MLR model, while the validation component was utilized to assess model performance. All MLR outputs, including plots and summary statistics, refer only to the validation component. The model training and validation process was performed 100

times for each model, with each iteration involving a different random partitioning of the training and validation data sets.

3. Results

Here we explore the results of two flux calculations to estimate OC sedimentation from global sedimentary samples (Figure 1). We refer to these OC sedimentation estimates as the *total* OC sedimentation (e.g., marine and terrestrial Section 3.1.1) and the *marine* OC sedimentation (Section 3.1.2; e.g., screening data to determine whether OC sedimentation is primarily of terrestrial or marine origin).

3.1. Organic Carbon Sedimentation Along the Continental Margins

3.1.1. Regionally and Bathymetrically Constrained Flux Estimate

To mitigate interpolation or extrapolation between hydrographically distinct regions, we divided the global margins into 30 regions based on geography, bathymetry (i.e., 0–1,000 and 1,000–1,500 m bins), and data density for a total of 60 bins (Figure 2). Regions were defined as close as possible to the regions defined by Jahnke (2010), where the margins were separated into five categories: polar, subpolar, monsoonal, tropical, eastern boundary current, and western boundary current. The polar regions, which include the Arctic and the region near Antarctica, were defined by ecosystems that have extreme seasonality (e.g., light limitation and have ice-cover for a significant part of the year). The sub-polar margins are in the high-latitude regions, which lie between the polar regions and the east and western-boundary current regions. The Western and Eastern Boundary currents are regions where water flows parallel to the margins, where west coast margins (or Eastern Boundary currents) are characterized by upwelling and subsurface oxygen minima. The monsoonal margins are regions that are affected by monsoonal wind patterns. Here, and in Jahnke (2010), the monsoonal margins are only based in the Northern Indian Ocean. Finally, the tropical margins are located at the low latitudes and are found roughly between 15° S and 15° N. For a detailed breakdown of these regions, the reader is referred to Jahnke (2010).

After breaking our margin area into these five categories, we considered data density in defining our regions. For example, instead of grouping the entire coast of western North America as the same eastern boundary current area, we split our data set into three regions—the Gulf of Alaska, California margin to Canada, and Mexico to Panama. These splits are possible because of the higher data density in these regions. Additionally, regions with low data density were necessarily defined by the location of samples. Once the region and bins were defined, we interpolated OC sedimentation separately within the two bins in each region. We created the bathymetry bins by clipping based on the bathymetry from Smith and Sandwell (1997). This method divided the data into two bins: 0–1,000 and 1,000–1,500 m. This grouping limited the effects of the low OC flux values at deeper depths from being extrapolated up-slope and artificially reducing the margin flux. Similarly, it prevented the shallow points from being extrapolated far down the slope, which would artificially inflate the margin fluxes. Though increasing the number of depth bins reduced vertical extrapolation, this came at the cost of diminishing data density in certain bins and in several regions. We found that using two depth bins optimized the tradeoff between minimizing vertical extrapolation and maintaining high data density; while more bins would be preferable, this is not possible without additional data. Although we utilized a seafloor data set (Smith & Sandwell, 1997) to avoid projecting over land masses, some inland bodies of water might have been included if their bathymetry was part of the data set. However, we anticipate the impact of these regions is negligible because they represent minimal area and are largely connected to the open ocean.

We summed the values for OC sedimentation in each bin and repeated the steps for each of the 30 regions. The steps for defining regions, bathymetry, and interpolation are shown in Figures 3a–3f. This approach allowed us to calculate regional and margin-wide flux estimates (Table 2). This regionally and bathymetrically constrained flux method is our preferred approach as it accounts for bathymetry and prevents extrapolations across dissimilar regions. This method yields a global margin OC sedimentation of 23.2 ± 3.5 Tmol year^{-1}. Since IDW does not permit direct estimation of uncertainty, our uncertainties were derived using a resampling analysis, described in Sections 3.1.2 and 3.2.

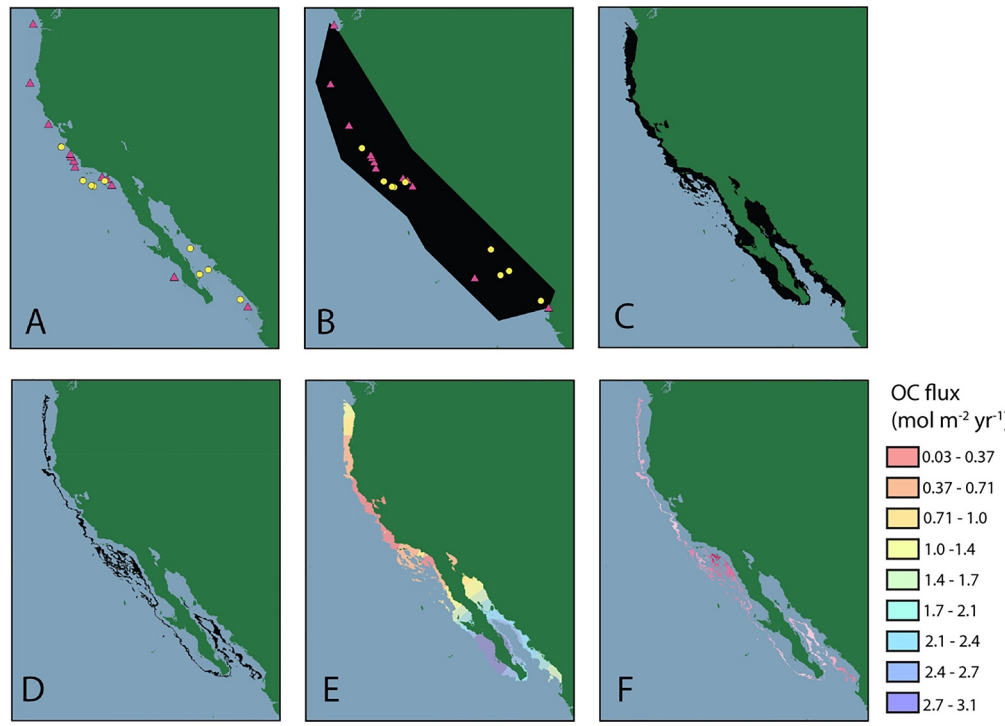

Figure 3. Maps of the California Margin (region b) illustrating the workflow of creating depth bins and the result of interpolating between data points. (a) Pink triangles indicate data between 0 and 1,000 m water depth and yellow circles are between 1,000 and 1,500 m, (b) regions of interest clipped around the data, (c) seafloor area from 0 to 1,000 m water depth within the regionally clipped area, (d) seafloor area from 1,000 to 1,500 m water depth within the regionally clipped area, (e) interpolated organic carbon (OC) fluxes within the 0–1,000-m depth bin, (f) interpolated OC fluxes within the 1,000–1,500-m depth bin. Final values were ascertained by summing the fluxes in each region. This process was repeated for each region of interest.

3.1.2. Regionally and Bathymetrically Constrained Flux Estimate for Marine OC

The bottom-up approach described in Section 3.1.1 provides an estimate of the flux of OC sedimented in margin environments, including both autochthonous and allochthonous sources. However, only the autochthonous fraction is relevant for constraining the magnitude and efficiency of the ocean's biological carbon pump. Therefore, in this second method, we separated the fraction of OC sedimentation derived from primarily marine sources versus those from terrestrial inputs, thus allowing us to estimate autochthonous OC sedimentation (Figure 4). As described in detail in the methods section, we filtered out sediments with a measured C:N > 8 or $\delta^{13}C < -23‰$. While this method allowed for a more accurate estimation of marine OC sedimentation, the screening removed around 15% of the data, thus leading to regions with insufficient data in either the deep (1,000–1,500 m) or shallow (0–1,000 m) bins to interpolate within each region. We leveraged the patterns observed in high-data-density regions to make a marine OC sedimentation estimation in these low-data-density bins. We selected six regions with high-density data coverage, contrasting hydrography, and water column OC flux attenuation and evaluated the relative OC sedimentation fluxes between the deep and shallow bins. The six regions we examined in detail were in the Northeast Pacific (Region b), the Southeast Pacific (Region f), the Northwest Atlantic (Region k), the Northeast Atlantic (Region n), and the Arctic (Regions ε and l; e.g., Figure 2, Table 3).

We observed similar ratios of OC sedimentation between shallow and deep bins, ranging from 7.8 to 16.4 (Table 3), despite substantial biogeochemical and hydrographic differences between regions. Since OC sedimentation exhibits systematic variations with respect to water depth, we developed a Monte Carlo method to estimate OC sedimentation in regions with limited data coverage. This approach involved randomly removing data from two of the six regions' shallow or deep bins while preserving the remaining data. Uncertainties in OC sedimentation of the remaining four shallow sites were introduced by assigning new estimates within 15% of the

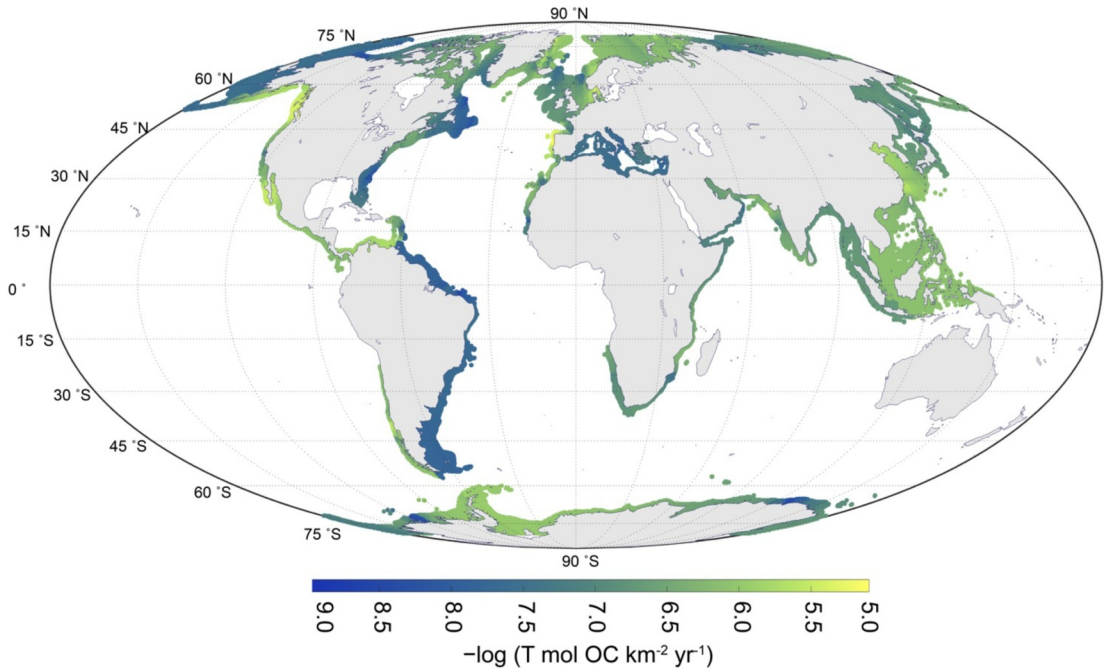

Figure 4. Marine organic carbon (OC) sedimentation flux across the globe along the margins. Generally, higher OC deposition rates are found in the Northeast Pacific and the West Equatorial Pacific Oceans. Interestingly, elevated OC rates were also observed in parts off of the coast of Antarctica and the Arctic Ocean. Relatively low OC fluxes define the western Atlantic margins. Regions without shading used previously tabulated estimates (Jahnke, 2010).

reported values, which accounts for uncertainties in MAR and OC measurements. This process was repeated 500,000 times for the shallow bin and the resulting predictions consistently reproduced the known values within their uncertainties. We find that the mean ratio of shallow-to-deep fluxes is 12.7 ± 1.1 (1 SD, Figure 5). This value agrees well with a separate bootstrapping analysis of the same data that does not prescribe uncertainties, which yielded a ratio of 12.6 ± 1.2 (1 SD).

To account for uncertainties in high-density data areas where applying a sedimentation ratio is not needed, we imposed a 15% uncertainty on each sedimentation estimate. Thus, OC fluxes in every single region and bin have individually assigned uncertainties, which allows us to calculate a marine-dominated OC sedimentation between 16.4 and 22.5 Tmol year^{-1}. Our best marine estimate, using a shallow-to-deep OC sedimentation ratio of 12.7, is 19.4 Tmol year^{-1}. Given that our best estimate for total (i.e., marine *and* terrestrial) OC sedimentation is 23.2 Tmol OC year^{-1}, it is evident that the marine flux accounts for the majority of total OC sedimentation globally. The fluxes for each region are given in Table 4.

As a validation check, we compared one of our flux estimates derived using the ratio value to a recent study that estimated the OC accumulation flux in the North Sea using a machine-learning method. This study suggests that

Table 3
Regions With High Marine Data Density

Coastal region	Basin	Total area (km^2)	Total area (km^2) 0–1,000 m	Total area (km^2) 1,000–1,500 m	Sedimentation rate (mol m^{-2} year^{-1}) 0–1,000 m	Sedimentation rate (mol m^{-2} year^{-1}) 1,000–1,500 m	Total sedimentation (Tmol OC year^{-1})	Ratio
b	NE Pacific	4.20E+05	3.32E+05	8.90E+04	1.51	0.13	0.51	11.44
f	SE Pacific	3.10E+05	2.66E+05	3.37E+04	0.85	0.06	0.23	13.60
k	NW Atlantic	1.70E+06	1.79E+06	1.21E+05	0.08	0.01	0.14	7.80
ε	Arctic	8.41E+06	8.11E+06	2.98E+05	0.39	0.03	3.16	14.09
l	Arctic	9.84E+05	7.48E+05	2.36E+05	1.19	0.10	0.91	11.34
n	NE Atlantic	5.08E+05	4.23E+05	8.50E+04	0.86	0.05	0.37	16.44

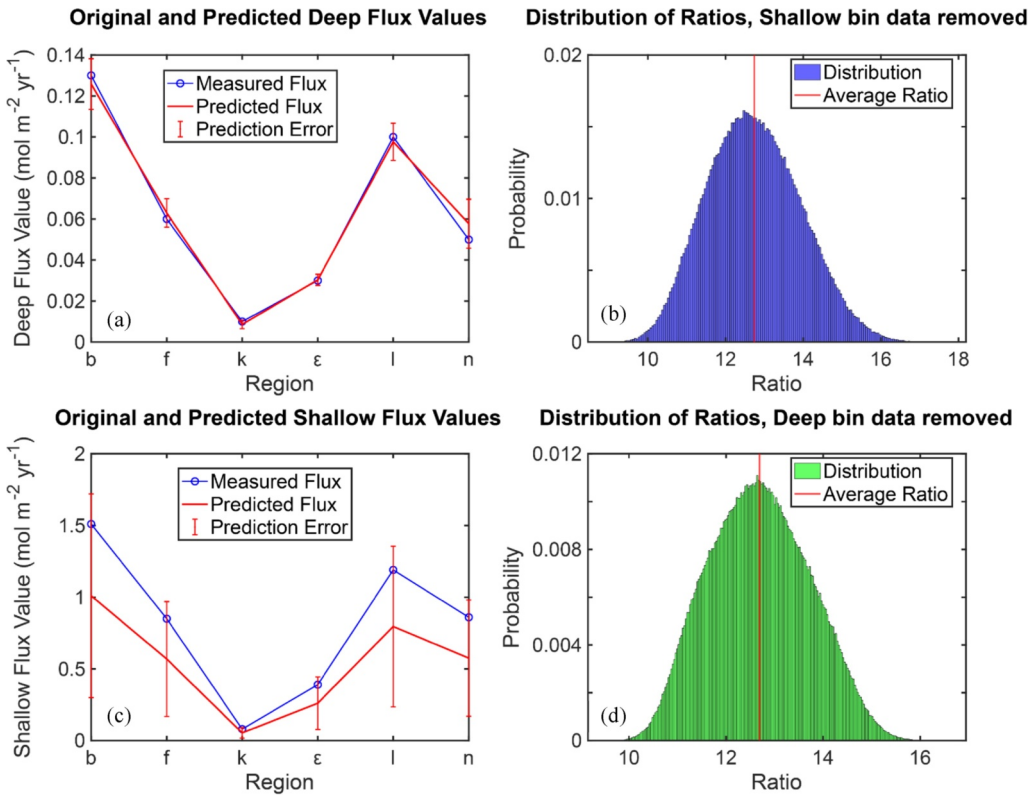

Figure 5. Uncertainty analysis on the ratio extrapolation method, (a, c) show the measured flux from the test sites against the predicted values when they are removed and subsequently predicted using the relationships in the remaining data. Panels (b, d) show a histogram of the distribution of the ratios between the shallow and the deep bins. The average ratio is 12.7 with a standard deviation of 1.1 (n = 500,000).

0.12 ± 0.17 Tmol C year^{-1} reaches the sediment in the North Sea and Skagerrak, with most of the sedimentation occurring in the Norwegian Trough. Using our mean sedimentation estimate in this region (i.e., region m, ratio at 12.7, 0.14 mol m^{-2} year^{-1}) and applying it to the area covered in that study (~560,000 km^2), we get an estimate of ≈0.08 Tmol C year^{-1}, which is in good agreement with the machine-learning method. It is important to note that each of these regional environments has important geographic textures to consider, resulting in heterogeneous OC arrival to the seafloor across the region. Despite this heterogeneity, our methods are still able to broadly replicate the detailed regional estimate. The global OC sedimentation patterns are shown in Figure 4. Generally, the highest marine OC fluxes are found in the East Pacific, the West Indian, and the Arabian Sea, with some elevated OC sedimentation in parts of the Arctic and Equatorial Pacific. The Atlantic generally shows the lowest OC sedimentation rates.

3.2. Multiple Linear Regression Modeling

Having derived a global OC sedimentation estimate using IDW, we employed statistical modeling to determine its predictability and identify the principal controlling factors. We achieved this using a series of MLR models that utilize the 459 OC sedimentation data that have complete records for all 12 predictor variables.

A total of 4,095 models were trained and we assessed model performance using standard metrics such as the Coefficient of Determination (R^2) and Mean Absolute Percentage Error (MAPE; Table S3 in Supporting Information S3). We found that trained model performance tended to plateau at an R^2 of ≈0.55, regardless of the number of features. We also observed that the R^2 of trained models tended to fall into one of three distinct populations: those with R^2 between 0.53 and 0.55, those with R^2 between 0.42 and 0.47, and those with R^2 between −0.03 and 0.23 (Figure 6). The first population included the 1,024 models where both depth and BWO were predictors; the second group comprised the 1,024 models where, regardless of any other features, depth was

Table 4
Marine-Only Organic Carbon Flux

General region	Figure code	Area in km^2 (0–1,000 m)	Area in km^2 (1,000–1,500 m)	Max flux (mol m^{-2} year^{-1})	Min flux (mol m^{-2} year^{-1})	Max (Tmol year^{-1})	Min (Tmol year^{-1})	Method	Bin with sufficient data density
NE Pacific	a	5.74E+05	3.08E+04	2.28	1.69	1.38	1.02	Ratio	0–1,000
NE Pacific	b	3.32E+05	6.96E+04	1.46	1.08	0.59	0.43	Binned	
NE Pacific	c	2.16E+05	5.28E+04	0.81	0.60	0.22	0.16	Ratio	0–1,000
SE Pacific	e	2.27E+05	6.63E+04	2.04	1.27	0.60	0.37	Ratio	1,000–1,500
SE Pacific	f	2.66E+05	3.37E+04	0.88	0.65	0.26	0.19	Binned	
SW Atlantic	g	1.79E+06	1.69E+05	0.26	0.16	0.51	0.32	Ratio	1,000–1,500
SW Atlantic	h	6.50E+05	8.43E+04	0.23	0.14	0.17	0.10	Ratio	1,000–1,500
W. Equ. Atlantic	i	2.94E+05	1.01E+05	0.17	0.17	0.07	0.12	Jahnke	NA
Gulf of Mexico	j	1.02E+06	2.17E+05	0.17	0.17	0.28	0.28	Jahnke	NA
NW Atlantic	k	1.79E+06	1.21E+05	0.08	0.06	0.16	0.12	Binned	
Arctic	l	7.48E+05	2.36E+05	1.07	0.79	1.05	0.78	Binned	
NE Atlantic	m	1.81E+06	3.52E+05	0.17	0.10	0.36	0.23	Ratio	1,000–1,500
NE Atlantic	n	4.23E+05	8.50E+04	0.83	0.61	0.42	0.31	Binned	
SE Atlantic	o	4.83E+05	9.44E+04	0.51	0.51	0.22	0.22	Jahnke	
SE Atlantic	p	3.98E+05	5.98E+04	0.60	0.38	0.28	0.17	Ratio	1,000–1,500
EW Indian	q	4.82E+05	1.75E+05	1.46	0.91	0.96	0.60	Ratio	1,000–1,500
Red Sea	r	3.99E+05	5.59E+04	0.02	0.01	0.01	0.01	Ratio	0–1,000
Black Sea	s	2.08E+05	3.39E+04	0.24	0.18	0.06	0.04	Ratio	0–1,000
W Arabian Sea	t	3.61E+05	2.65E+04	0.25	0.19	0.10	0.07	Ratio	0–1,000
E Arabian Sea	u	4.47E+05	7.36E+04	1.57	0.98	0.82	0.51	Ratio	1,000–1,500
Bay of Bengal	v	1.29E+06	2.31E+05	0.19	0.14	0.29	0.21	Ratio	0–1,000
Australia (West)	w	5.81E+05	1.79E+05	0.12	0.12	0.09	0.09	Jahnke	NA
Australia (South)	x	5.75E+05	5.69E+04	0.21	0.21	0.08	0.08	Jahnke	NA
Australia (East)	y	7.20E+05	1.40E+05	0.23	0.23	0.2	0.20	Jahnke	NA
Australia (Tropical)	z	1.33E+06	2.49E+04	0.25	0.25	0.45	0.45	Jahnke	NA
W Equ. Pacific	α	4.50E+06	5.07E+05	0.88	0.65	4.40	3.25	Ratio	0–1,000
NW Pacific	β	2.03E+06	4.83E+05	0.63	0.39	1.59	0.99	Ratio	1,000–1,500
S Pacific	ɣ	1.03E+06	5.81E+05	0.26	0.19	0.42	0.31	Binned	
Antarctic	δ	4.03E+06	3.40E+05	0.63	0.46	2.73	2.02	Binned	
Arctic	ε	8.11E+06	2.98E+05	0.43	0.32	3.64	2.69	Binned	
NE Pacific	ζ	2.65E+04	2.78E+04	0.02	0.01	0.00	0.00	Ratio	0–1,000
Med. Sea	ϑ	1.07E+06	2.27E+05	0.05	0.03	0.06	0.04	Binned	
Sum						**22.45**	**16.40**		

included as a predictor and BWO was not; and, the third group consisted of the 2,047 models that did not encode depth, although half of these models included BWO as a predictor.

We then conducted a feature significance analysis to identify the features exerting the most influence on predicting log-transformed OC sedimentation. By comparing the R^2 values of all 2,048 models encoding a feature against those 2,047 that did not, we calculated the absolute and relative changes in R^2. Additionally, we performed a two-way, unpaired heteroscedastic *t*-test and reported the resultant *p*-values. This analysis highlighted the importance of individual features on model performance and their statistical significance. Including depth as a predictor improved R^2 by an average of 115%, establishing it as the strongest predictor tested. Following depth, BWO also significantly improves R^2 by 21.3%. Other statistically significant predictors included: BWT (7.7%

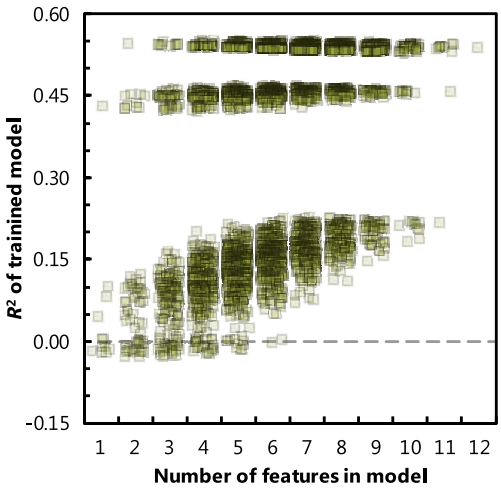

Figure 6. Performance of the multiple linear regression (MLR) models as a function of their complexity. The figure shows the R^2 between predictions and observations of each MLR model as a function of the number of features used to train that model. The models fall into three populations based on their R^2: those with values between 0.53 and 0.55, those with R^2 between 0.42 and 0.47, and those with R^2 between −0.03 and 0.23. The highest R^2 group comprises models that include both depth and bottom-water oxygen (BWO). The middle group consists of models that include depth (excluding those that are in the highest R^2 model group), but not BWO. The lowest R^2 group contains models that do not incorporate depth, though they may encode BWO.

improvement), MLD (7.1%), SWO (7.0%), sea-surface temperature (4.7%), and surface silicate concentrations (4.6%). Chlorophyll-a, surface phosphate, and surface nitrate exhibited modest model improvements (ranging from 0.6% to 1.7%), though these effects lacked statistical significance at the 95% level. Notably, the inclusion of latitude or longitude in an MLR model marginally degraded model performance, though these effects were also statistically insignificant (Table S3 in Supporting Information S3).

Figure 7 illustrates a comparison between predicted and observed log-transformed OC sedimentation for three selected MLR models. These accurate models were chosen for visualization for the following reasons: Model #1796 incorporates all seven features that exhibit statistically significant enhancements to model outputs, achieving an $R^2 \approx 0.54$. Model #4052 exhibits similar performance to the best MLR models in our analysis, with an $R^2 \approx 0.55$, though this is achieved with only three features: depth, BWO, and BWT. Lastly, Model #4060 achieves an $R^2 \approx 0.54$ but utilizes only two features—depth and BWO. With the exception of the coefficient for MLD in Model #1796, the coefficients for all terms in these three MLR models were negative, implying that an increase in any parameter would be predicted to drive a decrease in OC sedimentation.

Although MLR represents a simple form of statistical modeling that assumes linear relationships without interactions between variables, our analysis suggests that even relatively straightforward models comprising only a few features can effectively capture a significant portion of the variability within the underlying OC sedimentation data.

4. Discussion

4.1. Magnitude of OC Sedimentation

4.1.1. Comparison With Prior Flux Estimates and Global OC Sedimentation Patterns

Our regionally and bathymetrically constrained flux estimate places marine OC sedimentation between 16.4 and 22.5 Tmol OC $year^{-1}$. This range compares well with several top-down estimates established by previous studies reporting 15.6 (Jahnke, 2010) and 24.2 Tmol OC $year^{-1}$ (Dunne et al., 2007). Although Dunne et al. (2007) and Jahnke (2010) report their values as burial fluxes, we compare them to our OC sedimentation estimates because true burial is inherently unknowable. Regardless of the differences due to how burial is defined, the broad convergence of these estimates bolsters our confidence that the uncertainties inherent to each approach do not compromise the ability to accurately determine OC sedimentation to recent sediments.

Globally, regions with the highest marine OC sedimentation are found in the East Pacific, West Indian Ocean, and the Arabian Sea. Conversely, the lowest fluxes are found in the Red Sea and the North Atlantic. Elevated OC sedimentation is also noted in certain parts of the Arctic and Antarctic. The Arctic is characterized by broad, shallow continental shelves, while the Antarctic shelf, although deeper than the Arctic, extends significantly below continentally-based ice sheets. Additionally, the colder bottom waters in these polar regions reduce the rate of heterotrophic respiration of OC compared to the warmer bottom waters in the low-latitudes.

4.1.2. Efficiency of the Biological Carbon Pump

We can use our OC flux to determine the overall long-term (i.e., millennial) efficiency of the marine biological carbon pump. This calculation is based on the fraction of NPP that reaches the seafloor rather than nutrient use efficiency (as in Volk & Hoffert, 1985). Marine biogeochemical models estimate that between 800 and 850 Tmol C $year^{-1}$ are exported as particulate OC below the euphotic zone (Jin et al., 2006; Nowicki et al., 2022), roughly equivalent to current anthropogenic CO_2 emissions of ≈800 Tmol C $year^{-1}$ (Friedlingstein et al., 2022). Using our predominantly-marine margin OC sedimentation estimate of 19.4 Tmol $year^{-1}$ and combining it with OC sedimentation in the deep sea, we can calculate the total sedimentation of OC in the ocean. While recognizing that the deep-sea estimates are not perfectly aligned with our own due to differences in water depths, we choose a

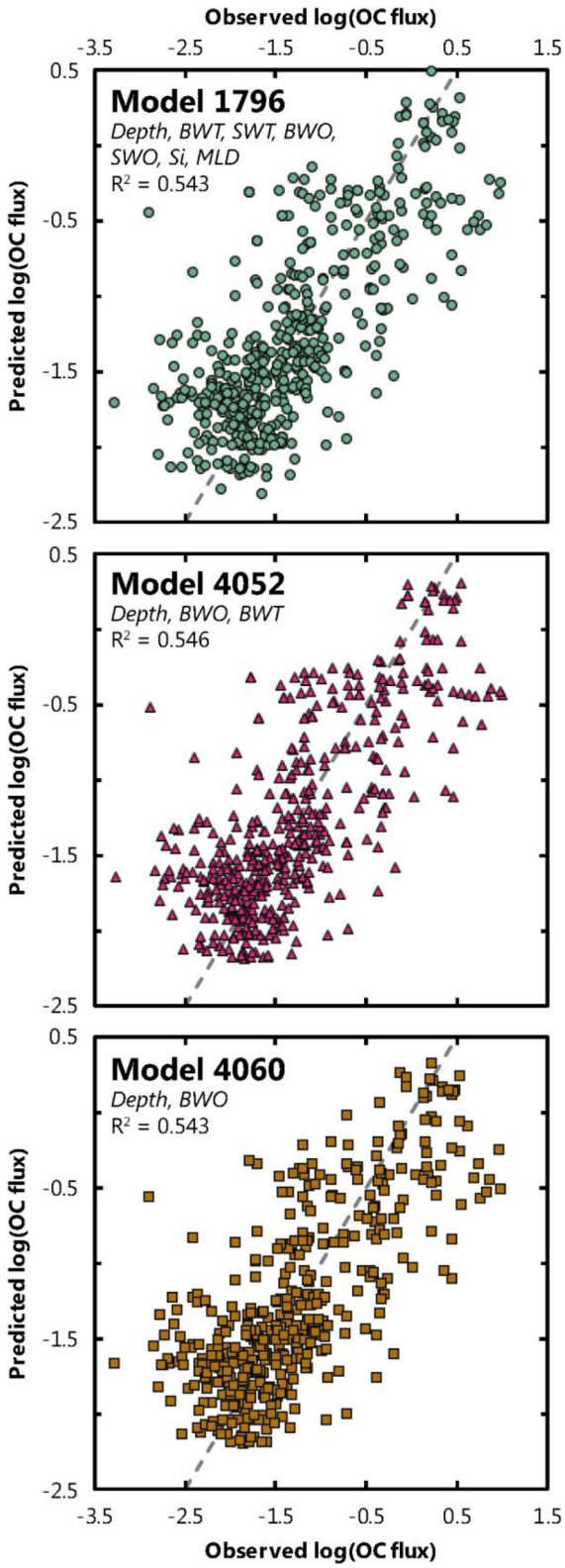

Figure 7. Relationship between predicted and observed log-transformed organic carbon (OC) sedimentation for models 1796 (top), 4052 (middle) and 4060 (bottom). The dashed line indicates a 1:1 relationship.

middle value of 1.6 ± 0.5 Tmol C year^{-1} (Hayes et al., 2021), which is within the uncertainty of estimates deeper than 1,000 m (1.7 ± 0.5 Tmol C year^{-1}) or deeper than 2,000 m (1.4 ± 0.4 Tmol C year^{-1}; Hayes et al., 2021). The total flux is then calculated as 21 ± 3.1 Tmol OC year^{-1}. Thus, we estimate that between 2.2% and 3.0% of the organic matter exported below the euphotic zone escapes remineralization and is ultimately sedimented. This aligns well with previous literature estimates (e.g., Behrenfeld & Falkowski, 1997; Iversen, 2023; Jahnke, 1996; Sarmiento & Gruber, 2006) and supports the robustness of our findings.

Additionally, we estimate that approximately 92% of OC sedimentation occurs at water depths shallower than 1,500 m. This finding provides critical values for determining the flux of OC sedimentation and contextualizes the role marine sediments can play in sequestering anthropogenic carbon. Our work also identifies the factors governing OC sedimentation and highlights the geographic regions contributing most significantly to OC sedimentation during the Holocene.

4.2. Drivers of OC Flux Variability

4.2.1. The Role of Bottom Water Oxygen on OC Sedimentation

Our analysis of OC sedimentation as a function of BWO concentrations, extracted from the WOA18, indicates that regions with bottom water [O_2] in the range of 100–150 μM exhibit the highest OC sedimentation per unit area (Figure 8c). We also find that 43% of OC sedimentation along the margins occurs in regions with a bottom water [O_2] lower than 200 μM, while approximately 57% of OC sedimentation occurs in regions with bottom water [O_2] between 200 and 400 μM (Figure 8b). Most of the OC sedimentation under these higher oxygen conditions occurs in the Arctic and Southern Oceans, which typically have lower bottom-water temperatures. Regions with bottom water [O_2] <50 μM, typically considered hotspots of OC sedimentation, constitute <4% of global margin OC sedimentation (Figure 8b). This low percentage is attributed to both the limited areal extent of such regions and the relatively minor role that bottom water [O_2] plays in influencing OC sedimentation globally. Thus, we do not see significant evidence within our data to suggest that OC sedimentation is disproportionately higher or more efficient in low-oxygen regions of the ocean. Instead, each region characterized by a similar range of BWO exhibits relatively similar OC sedimentation when normalized by area (Figure 8). A recent study of particulate organic matter distributions observed similar patterns in the water column, noting that remineralization rates did not display a strong dependence on ambient [O_2] (Amaral et al., 2024). It is important to note that because we grouped the BWO values into large bins (0–50 μM O_2), we do not expect seasonal variations to substantially impact the overall bottom water concentrations. Collectively, these results suggest that the oxygen content of bottom waters plays a relatively minor role in determining OC sedimentation on a global scale. This finding is supported by our MLR modeling, which showed that adding bottom water [O_2] as a predictor resulted in only a modest improvement in MLR model performance compared to depth (Section 3.2).

One possibility for the low predictive power of BWO for OC sedimentation may be due to the presence of other electron acceptors in sediment porewaters. While oxygen has the most negative Gibbs free energy associated with it, many other electron acceptors also participate in organic matter

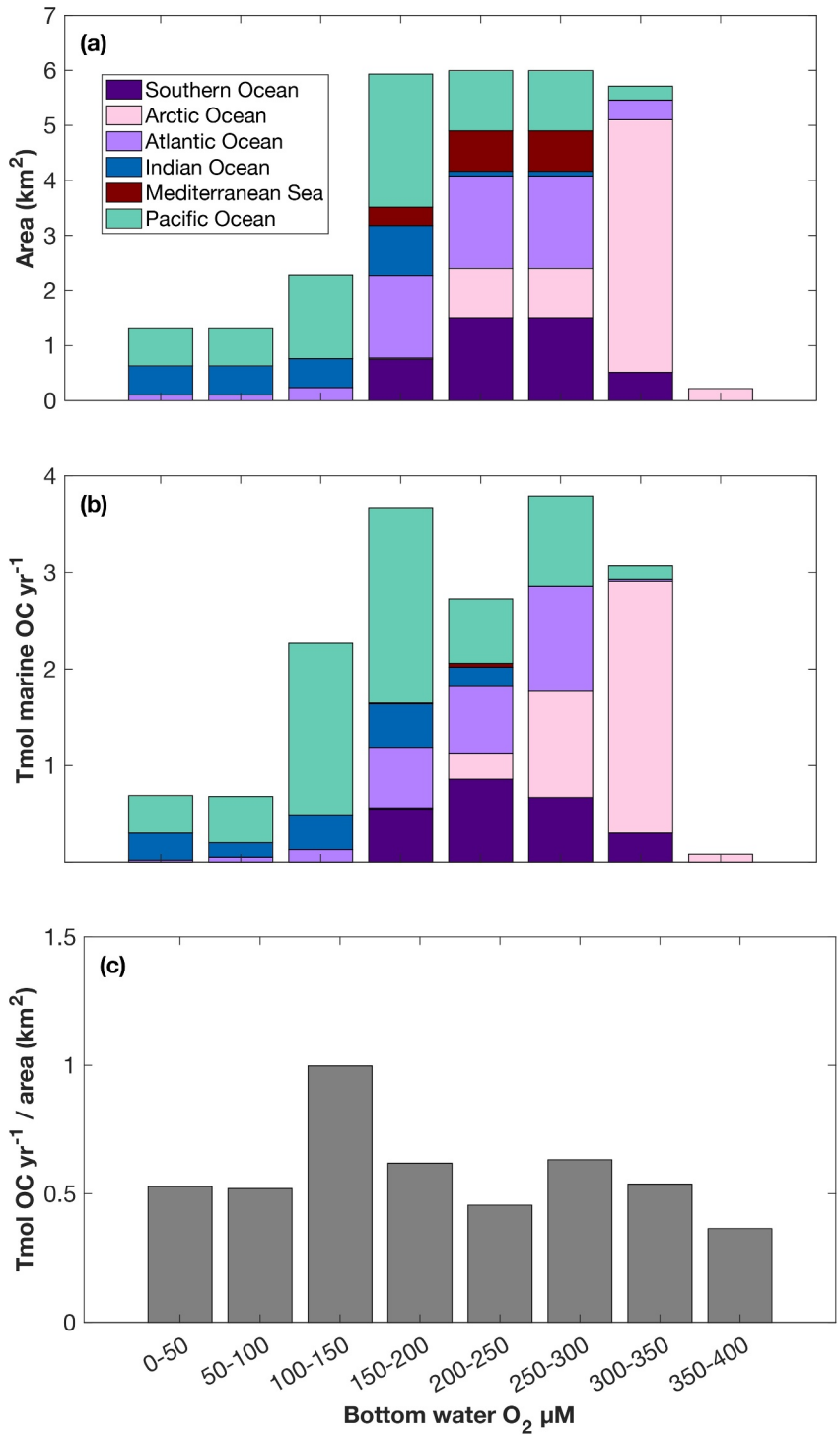

Figure 8. Marine organic carbon (OC) fluxes (a), seafloor area (b), and area-normalized OC sedimentation (c) shown as a function of water depth.

degradation in sediment, including NO_3^-, Mn(IV), Fe(III), SO_4^{2-}, and CO_2 (e.g., Claypool & Kaplan, 1974; Froelich et al., 1979; Stumm & Morgan, 1996). Although many studies suggest that the presence of O_2 typically enhances OC degradation, several studies argue that the presence of oxygen in porewaters is not the critical factor for determining POC reactivity (Hulthe et al., 1998; Pedersen & Calvert, 1990). Indeed, studies have suggested

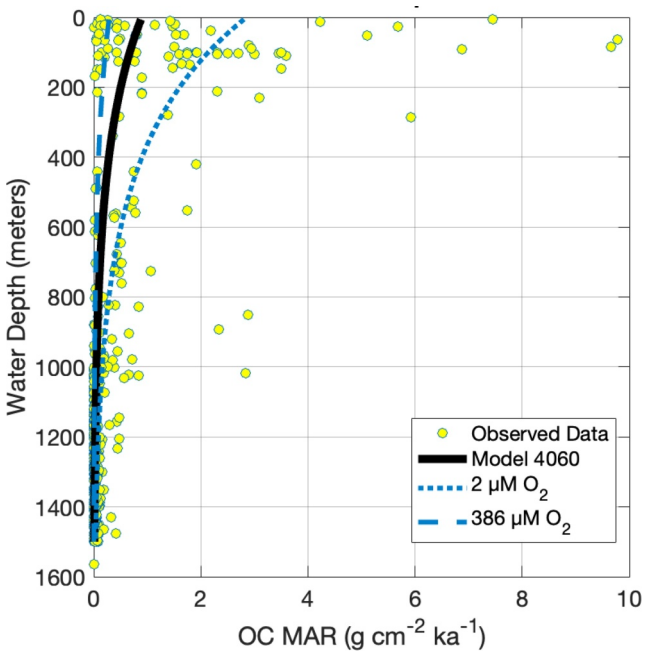

Figure 9. Observed organic carbon (OC) sedimentation values are plotted against their bathymetry in the yellow points. The modeled data are shown for Model 4060 (solid line). The dashed lines show the model results assuming a BWO value of either 2 μM or 386 μM.

that POC degradation rates in anoxic regions can be equal (Henrichs & Reeburgh, 1987; Kristensen & Holmer, 2001) or even exceed POC reactivity in oxic regions (D'Hondt et al., 2015; Røy et al., 2012). Our results align with this perspective, indicating that while low oxygen is a predictor for OC sedimentation, it does not appear to exert the primary influence.

However, it is crucial to note that our study focused on BWO, not porewater oxygen levels. In regions with high OC fluxes, such as along the margins, the oxygen penetration depth into the sediment could be very small (Glud, 2008). Thus, sediment that underlies oxic bottom water may be mostly anoxic. Unfortunately, there are no gridded data sets of porewater oxygen levels to determine the role that porewater oxygen concentrations play in POC reactivity in the sediment. Regardless of the differences between porewater oxygen and BWO, our data suggest that water column oxygen concentrations may not exert as much influence as previously thought. This insight is pivotal in the context of proposed carbon dioxide removal projects aiming to sequester carbon by depositing organic matter in low-oxygen or anoxic regions (e.g., Raven et al., 2024). If such projects rely on BWO concentrations for site selection, they may not achieve the anticipated long-term carbon sequestration results, as our findings indicate that there may only be moderate gains from sinking carbon in anoxic regions compared to oxic ones. Scaling up carbon sequestration efforts in sediments demands more investigation.

4.2.2. Water Depth as the Dominant Control on OC Sedimentation

We now turn to identifying the primary influences on OC sedimentation, with our MLR analysis underscoring water depth as the most influential predictor. Indeed, a model utilizing depth as the sole predictor (Model #4092) achieves an R^2 of 0.43, equivalent to 78% of the variance that can be explained by the MLR approach. While water depth emerges as the primary control on OC sedimentation in our MLR, this variable likely acts as a proxy for a multitude of physical, chemical, and biological processes that operate at different depths.

Visual inspection of the vertical structure of OC sedimentation data reveals that the highest flux values predominantly occur in continental shelf waters (i.e., depths shallower than 200 m; Figure 9). These shallower regions also tend to exhibit the most variance, with the top 200 m of the data set encapsulating the entire range of OC sedimentation fluxes. In contrast, deeper depths demonstrate lower OC sedimentation and significantly reduced variance. One reason for the high variance along the shelf is that these regions are characterized by episodic sedimentation of OC, periods of non-sedimentation, and—in shallow areas—erosion. The shelf is also influenced by processes occurring along the land-to-ocean aquatic continuum, a series of "loops" that recycle and transform OC as it is transported from soils to the open ocean (e.g., Regnier et al., 2022). The final loop of this continuum involves the continental shelf, where significant reprocessing occurs. Beyond the shelf lies the open ocean, which then acts as the terminal sink for exported organic matter.

Additionally, the shallow ocean typically hosts both production *and* regeneration of OC. This can lead to high OC flux variability since it depends on two processes—OC formation and regeneration—that both exhibit heterogeneity. In contrast, below 200 m, there is very little autotrophic production of OC. Consequently, the dominant control on OC fluxes below 200 m is regeneration. Over long-length scales, this regeneration process tends to follow a consistent "Martin-like relationship," regardless of whether the degradation is mediated by bacteria or zooplankton (e.g., Steinberg et al., 2008). Thus, our results indicate that regions with the highest OC flux uncertainty are those closest to the land, highlighting such areas as a priority for further study. This is particularly important as human-driven changes to marine environments are most acute in these regions (Regnier et al., 2022).

It is important to note that other forms of OC preservation may also be significant in decoupling OC production from sedimentation. While water depth is the primary factor identified here, this term encompasses both respiration in the water column and early diagenetic reactions taking place at the seafloor. The latter likely contributes as much, if not more, to OC remineralization than pelagic processes (e.g., Berner, 1980). However, given the nature of our statistical approach, it is challenging to determine the relative importance of pelagic versus benthic

remineralization in decoupling OC production from sedimentation. We encourage future studies to investigate this distinction, as it will shed light on the ultimate controls on OC preservation in marine sediments.

4.2.3. Primary Productivity Is Not Strongly Correlated With OC Sedimentation

Notably, our findings reveal that OC sedimentation has no statistically significant relationship with sea-surface chlorophyll-a concentrations, either alone or in concert with other predictors. To a first order, this finding implies that surface water productivity does not meaningfully influence the amount of OC ultimately sedimented on the seafloor. However, the challenges in accurately quantifying chlorophyll-a concentrations using satellite data—particularly the potential overestimation in near-shore environments due to increased particle loading—suggest that OC production might still have some influence on OC sedimentation. Future research may consider comparing derived rates of NPP or gross primary productivity with OC sedimentation, although some challenges remain in transforming pigment and chlorophyll measurements into rates (Westberry et al., 2023).

4.2.4. Other Considerations

Our MLR model only accounted for a fraction of the total variability in the data. This could be due to non-linear relationships between the 12 modeled parameters. However, it is also likely that additional parameters, which we were unable to model, play a role in determining OC sedimentation. We will briefly examine three potential parameters that could be important for OC sedimentation. First, the microbes that the OC encounters in the sediment could be important for determining OC reactivity. Cell abundances in all surface margin sediments are estimated to be between 10^8 and 10^{10} cells cm^{-3} (Kallmeyer et al., 2012) and certainly impact how much OC is remineralized in the sediment. Different sediment types have been shown to have distinct microbial communities (Orsi, 2018), which could explain differences in OC sedimentation. Second, there is a correlation between OC concentrations and mineral surface area (e.g., Keil et al., 1994; Mayer et al., 1985), with OC possibly being protected by minerals through mechanisms such as absorption in mineral micro-pores and co-precipitation with Fe-oxyhydroxides (La Rowe et al., 2020; Moore et al., 2023). Finally, the composition of organic matter may influence OC sedimentation. Particulate OC comprises a diverse array of chemical compounds, some of which are more reactive or recalcitrant than others. Although structure and composition offer insights into reactivity, identifying and classifying marine POC remains challenging, with a significant portion deemed "uncharacterizable" (e.g., Hedges et al., 2000). Despite this, studies indicate that weak bonds between monomers generally increase biopolymer reactivity (La Rowe et al., 2020; Tegelaar et al., 1989). Future research could focus on understanding the significance of each of these parameters more fully to improve the overall predictability of OC sedimentation and the factors that control it.

4.3. Quantifying Uncertainties and Utility of the Carbon Flux Estimate

While our bottom-up methodology offers valuable insights into sedimentary OC sedimentation, several limitations warrant consideration. These include potential oversampling of non-representative regions, low data density from areas underlying very shallow water depths, OC sedimentation attenuation with sediment age, challenges in assigning uncertainties, and inability to account for all processes affecting OC preservation. We explore these limitations and suggest that while these uncertainties will affect the *precision* of our estimates, they will have a minimal effect on their overall *accuracy*.

4.3.1. Inverse Distance Weighting Limitations

In this study, we opted to calculate global OC sedimentation using IDW, a method we selected for several reasons. Most significantly, this technique provides a straightforward and easily interpretable method for estimating OC sedimentation with conservative assumptions. However, IDW is not without limitations. One notable challenge is its reliance on a defined decorrelation length scale to interpolate between data points. As previously mentioned, this interpolation is based on values from neighboring points, prioritizing those physically closest to the gap (Section 2.2). Yet, this approach fails to account for seafloor heterogeneity. In regions with significant variations in topography or bottom water chemistry and biology, the decorrelation scale may be shorter than what IDW can accurately determine.

Addressing this challenge involves more data acquisition and employing more sophisticated methods in the future. Numerous factors, including geomorphological, geochemical, hydrographic, and biological factors, can

influence OC sedimentation over short distances (Levin & Sibuet, 2012). If these parameters are well-represented in a data set covering several relatively small regions in all of the basins that exhibit significant topographic variations, more advanced techniques such as machine learning could be used to interpolate between points more effectively, without relying only on proximity to existing measurements.

4.3.2. Sample Site Bias

Study site selection is often driven by the desire to study specific phenomena, such as low-oxygen environments, upwelling, cross-shelf transport, or ecology. Therefore, regions hosting unusual oceanographic phenomena may be overrepresented in our sample compilation. Constraining the uncertainty caused by this limitation is challenging since several factors influence site selection. However, when we compare the distribution of raw OC sedimentation data versus BWO, a phenomenon we expected to be oversampled, we find that the distribution is remarkably similar (Figure S1 in Supporting Information S2). Thus, while we recognize that a bias toward regions with unique depositional environments may influence our margin flux value, we do not believe the bias impacts the primary findings of the study.

However, one potential limitation that is challenging to quantify relates to the observation that portions of the shelf are characterized by little-to-no sedimentation, or even erosion, which our analysis does not include. This could lead to an overestimation of OC sedimentation. While certainly a limitation of our analysis, it is not currently feasible to incorporate this into our areas of modeling since very little is known about the spatial distribution of non-sedimentation and erosional environments on the continental margins. As new data become available for these regions, they can be added to our current framework to provide a more nuanced estimate of OC sedimentation.

4.3.3. Attenuation of OC Sedimentation With Depth

We recognize that a significant fraction of our compiled data comes from sediments underlying water columns deeper than 700 m (Tables S1 and S2 in Supporting Information S3). Pelagic OC fluxes generally attenuate according to a power law as a function of water depth (Martin et al., 1987). Thus, we may be underestimating the marine OC sedimentation to the margins by having only relatively few data from shallower water depths. If this problem were to persist in the sample sites, it could lead to OC sedimentation in shallow waters that are too low. This could result in an underestimate of the global marine OC sedimentation. However, the data that we do have for samples in less than 200 m of water depth span the full range of OC sedimentation (Figure 9), suggesting that we capture OC sedimentation across the entire range of potential values.

4.3.4. Carbon Sedimentation as a Function of Sediment Age and Oxidation Processes

In this study, we only included sediments deposited during the Holocene (i.e., 0–11 Kyr BP), which serves to eliminate the large changes in productivity and bottom-water conditions associated with the last glaciation and deglacial period (Jaccard & Galbraith, 2012). Although accumulation rates at any site may have changed somewhat over the Holocene, this period was generally stable with a climate relatively similar to modern and only minor changes in sea level (Stanford et al., 2011). Because we purposefully selected sediment cores with ages as close to modern as possible, we assume that the rates of OC sedimentation throughout the Holocene are similar to modern values.

Using samples sedimented over a wider timeframe presents another potential concern in that there is variability in sedimentary oxygen exposure time within the sediment. BWO does not reflect porewater oxygen concentrations, which may be important for controlling remineralization within the sediment itself. In many coastal regions, the sediment porewater becomes anoxic within the first few centimeters, but, in some sediments, oxygen penetration extends beyond the upper layers. In such environments, older sedimentary OC, subjected to prolonged oxidation, might better reflect long-term OC burial. Conversely, younger sediment may more closely resemble the OC rain rate, rather than that which is irreversibly buried. As previously highlighted, our OC sedimentation estimate represents the upper limit of burial flux and does not account for the potential cessation of post-sedimentation remineralization, though a recent study suggests no such cessation occurs (Rothman, 2024). Thus, our OC sedimentation estimate likely falls between the rain rate at the sediment-water interface and the true long-term burial flux. The ideal method to determine accurate OC burial involves integrating OC burial fluxes over the

last 11,000 years, necessitating OC accumulation rate estimates for each sample throughout that period, which is presently unfeasible for the samples used in this study.

4.3.5. Recommendations for Future Research

This study identifies several critical areas for future research. First, enhancing our ability to predict OC sedimentation demands increased sample collection, particularly in regions with sparse data coverage, shallow water depths, and areas subject to non-sedimentation and erosion. Expanding the data set would also enable researchers to explore OC sedimentation across a broader spectrum of depth bins. Additionally, further investigation is needed to understand the influence of factors that are challenging to quantify, such as microbial degradation of OC, mineral protection mechanisms, and the variable lability of OC in sediments. Lastly, we advocate for the adoption of more advanced statistical methods, such as machine learning, to more effectively interpolate between —and extrapolate beyond—existing data.

5. Conclusions

Organic carbon export to marine sediments removes carbon dioxide from the atmosphere on centennial-to-million-year timescales. Although several studies have combined measurements of sediments and modeling to estimate OC sedimentation in the deep sea, no such exercise has been undertaken along the continental margins, where most of global OC sedimentation is thought to occur. Here, we compiled OC flux data for Holocene sediments from the primary literature as well as the PANGAEA and IODP databases and used geospatial interpolation to produce a bottom-up estimate of the OC sedimentation along the margins. Our preferred estimate of marine margin OC sedimentation is 19.4 Tmol OC year^{-1}. Combined with previous estimates of deep-sea OC sedimentation of 1–2 Tmol C year^{-1}, we estimate the global *marine flux* over all water depths to be between 17.4 and 24.5 Tmol C year^{-1} (0.2–0.3 Pg C year^{-1}). Additionally, we estimate that the margins host a *total OC* sedimentation, including both marine-and terrestrial-sources, of 23.2 ± 3.5 Tmol C year^{-1}, resulting in a whole-ocean OC sedimentation estimate of 24.9 ± 3.6 Tmol C year^{-1}.

Our estimates compare reasonably well with previous top-down approaches and suggest that the efficiency of global OC export from the euphotic zone to the seafloor is between 2% and 3%. Contrary to the paradigm that OC sedimentation is strongly focused in low-oxygen regions, our data show that >95% of OC sedimentation occurs in regions with bottom water [O_2] ≥50 μM. Using multiple-linear regression analysis, we demonstrate that OC sedimentation primarily depends on the transit distance to the seafloor. Other factors tested, such as bottom-water [O_2], bottom water-temperature, and MLD, are of secondary importance. Notably, productivity in the surface ocean, as inferred from sea-surface chlorophyll concentrations, showed no significant relationship to OC sedimentation. Collectively, these findings highlight the importance of other factors, such as OC preservation, as the principal driver of OC sedimentation. Preservation is ultimately determined by a combination of pelagic remineralization and early diagenetic reactions occurring at the seafloor. However, our approach does not resolve the specific proportions of these two processes. Apportioning the relative magnitude of pelagic processes and benthic breakdown to total OC preservation is a significant and important challenge that would be greatly aided by additional depth-resolved sediment data and more advanced modeling.

The two methods used to explore OC fluxes in this study, IDW and MLR, provide initial insights and establish a baseline understanding of the data, while also highlighting certain limitations. Chief among the limitations is the low data density in certain regions of the ocean, such as the Australian margins and the Southeast Atlantic. While the statistical methods employed here were useful in identifying predictors of OC sedimentation, even our most robust MLR models explain only slightly more than half of the variance in the data. This suggests that there may be additional parameters that we did not test in our model that exert a strong control over OC sedimentation. Additionally, non-linear relationships between parameters, which cannot be detected using MLR without interaction terms, may also play an important role. Such processes could potentially be better addressed using more advanced statistical methods, such as machine learning, to create a more predictive model of global OC sedimentation.

Conflict of Interest

The authors declare no conflicts of interest relevant to this study.

Data Availability Statement

The data collected and generated in this manuscript are available at Mendeley Data, an open-source online data repository (Tegler, 2024). See references for links to data.

Acknowledgments

We acknowledge financial support from the U.S. National Science Foundation, specifically Graduate Research Fellowship #1122374 (awarded to L.A.T.), GEO-NERC 1948716 (to S.G.N.), OCE-1851309 (to V.G.), and OCE-2023456 (to T.J.H.). Additionally, T.J.H. recognizes support from the Woods Hole Oceanographic Institution's *Breene M. Kerr Early Career Scientist Endowment Fund*, the *Ocean and Climate Innovation Accelerator*, and the *Independent Research & Development Program*. We extend our gratitude to the two anonymous reviewers for their insightful and detailed comments, as well as to Nicolas Gruber for editorial oversight. We appreciate their efforts and recognize that our study has substantially improved as a result.

References

Amaral, V. J., Lam, P. J., Marchal, O., & Kenyon, J. A. (2024). Cycling rates of particulate organic carbon along the GEOTRACES Pacific meridional transect GP15. *Global Biogeochemical Cycles*, *38*(1), e2023GB007940. https://doi.org/10.1029/2023gb007940

Archer, D. E., Morford, J. L., & Emerson, S. R. (2002). A model of suboxic sedimentary diagenesis suitable for automatic tuning and gridded global domains. *Global Biogeochemical Cycles*, *16*(1), 17-1–17–21. https://doi.org/10.1029/2000gb001288

Arndt, S., Jørgensen, B. B., LaRowe, D. E., Middelburg, J. J., Pancost, R. D., & Regnier, P. (2013). Quantifying the degradation of organic matter in marine sediments: A review and synthesis. *Earth-Science Reviews*, *123*, 53–86. https://doi.org/10.1016/j.earscirev.2013.02.008

Atwood, T. B., Witt, A., Mayorga, J., Hammill, E., & Sala, E. (2020). Global patterns in marine sediment carbon stocks. *Frontiers in Marine Science*, *7*, 165. https://doi.org/10.3389/fmars.2020.00165

Bauer, J. E., Cai, W. J., Raymond, P. A., Bianchi, T. S., Hopkinson, C. S., & Regnier, P. A. (2013). The changing carbon cycle of the coastal ocean. *Nature*, *504*(7478), 61–70. https://doi.org/10.1038/nature12857

Behrenfeld, M. J., & Falkowski, P. G. (1997). A consumer's guide to phytoplankton primary productivity models. *Limnology & Oceanography*, *42*(7), 1479–1491. https://doi.org/10.4319/lo.1997.42.7.1479

Berner, R. A. (1980). *Early diagenesis: A theoretical approach*. (No. 1). Princeton University Press.

Berner, R. A. (1989). Biogeochemical cycles of carbon and sulfur and their effect on atmospheric oxygen over Phanerozoic time. *Global and Planetary Change*, *1*(1–2), 97–122. https://doi.org/10.1016/0921-8181(89)90018-0

Bianchi, T. S., Cui, X., Blair, N. E., Burdige, D. J., Eglinton, T. I., & Galy, V. (2018). Centers of organic carbon burial and oxidation at the land-ocean interface. *Organic Geochemistry*, *115*, 138–155. https://doi.org/10.1016/j.orggeochem.2017.09.008

Bradley, J. A., Hülse, D., LaRowe, D. E., & Arndt, S. (2022). Transfer efficiency of organic carbon in marine sediments. *Nature Communications*, *13*(1), 7297. https://doi.org/10.1038/s41467-022-35112-9

Burdige, D. J. (2007). Preservation of organic matter in marine sediments: Controls, mechanisms, and an imbalance in sediment organic carbon budgets? *Chemical Reviews*, *107*(2), 467–485. https://doi.org/10.1021/cr050347q

Cartapanis, O., Bianchi, D., Jaccard, S. L., & Galbraith, E. D. (2016). Global pulses of organic carbon burial in deep-sea sediments during glacial maxima. *Nature Communications*, *7*(1), 10796. https://doi.org/10.1038/ncomms10796

Claypool, G. E., & Kaplan, I. R. (1974). The origin and distribution of methane in marine sediments. In *Natural gases in marine sediments* (pp. 99–139).

D'Hondt, S., Inagaki, F., Zarikian, C. A., Abrams, L. J., Dubois, N., Engelhardt, T., et al. (2015). Presence of oxygen and aerobic communities from sea floor to basement in deep-sea sediments. *Nature Geoscience*, *8*(4), 299–304. https://doi.org/10.1038/ngeo2387

Diesing, M., Thorsnes, T., & Bjarnadóttir, L. R. (2021). Organic carbon densities and accumulation rates in surface sediments of the North Sea and Skagerrak. *Biogeosciences*, *18*(6), 2139–2160. https://doi.org/10.5194/bg-18-2139-2021

Dunne, J. P., Armstrong, R. A., Gnanadesikan, A., & Sarmiento, J. L. (2005). Empirical and mechanistic models for the particle export ratio. *Global Biogeochemical Cycles*, *19*(4), GB4026. https://doi.org/10.1029/2004gb002390

Dunne, J. P., Sarmiento, J. L., & Gnanadesikan, A. (2007). A synthesis of global particle export from the surface ocean and cycling through the ocean interior and on the seafloor. *Global Biogeochemical Cycles*, *21*(4), GB4006. https://doi.org/10.1029/2006gb002907

Eglinton, T. I., Galy, V. V., Hemingway, J. D., Feng, X., Bao, H., Blattmann, T. M., et al. (2021). Climate control on terrestrial biospheric carbon turnover. *Proceedings of the National Academy of Sciences*, *118*(8), e2011585118. https://doi.org/10.1073/pnas.2011585118

Falkowski, P. G., Barber, R. T., & Smetacek, V. (1998). Biogeochemical controls and feedbacks on ocean primary production. *Science*, *281*(5374), 200–206. https://doi.org/10.1126/science.281.5374.200

Friedlingstein, P., Jones, M. W., O'Sullivan, M., Andrew, R. M., Bakker, D. C. E., Hauck, J., et al. (2022). Global carbon budget 2021. *Earth System Science Data*, *4*(14), 1917–2005. https://doi.org/10.5194/essd-14-1917-2022

Froelich, P., Klinkhammer, G. P., Bender, M. L., Luedtke, N. A., Heath, G. R., Cullen, D., et al. (1979). Early oxidation of organic matter in pelagic sediments of the eastern equatorial Atlantic: Suboxic diagenesis. *Geochimica et Cosmochimica Acta*, *43*(7), 1075–1090. https://doi.org/10.1016/0016-7037(79)90095-4

Galy, V., Peucker-Ehrenbrink, B., & Eglinton, T. (2015). Global carbon export from the terrestrial biosphere controlled by erosion. *Nature*, *521*(7551), 204–207. https://doi.org/10.1038/nature14400

Gershanovich, D. E., Gorshkova, T. I., & Koniukhov, A. I. (1974). Organic matter in recent sediments of continental margins. In *Organic matter in recent and fossil sediments and methods of its investigation* (pp. 63–80).

Glud, R. N. (2008). Oxygen dynamics of marine sediments. *Marine Biology Research*, *4*(4), 243–289. https://doi.org/10.1080/17451000801888726

Hayes, C. T., Costa, K. M., Anderson, R. F., Calvo, E., Chase, Z., Demina, L. L., et al. (2021). Global ocean sediment composition and burial flux in the deep sea. *Global Biogeochemical Cycles*, *35*(4), e2020GB006769. https://doi.org/10.1029/2020gb006769

Hedges, J. I., Eglinton, G., Hatcher, P. G., Kirchman, D. L., Arnosti, C., Derenne, S., et al. (2000). The molecularly-uncharacterized component of nonliving organic matter in natural environments. *Organic Geochemistry*, *31*(10), 945–958. https://doi.org/10.1016/s0146-6380(00)00096-6

Hedges, J. I., & Keil, R. G. (1995). Sedimentary organic matter preservation: An assessment and speculative synthesis. *Marine Chemistry*, *49*(2–3), 81–115. https://doi.org/10.1016/0304-4203(95)00013-h

Hedges, J. I., Keil, R. G., & Benner, R. (1997). What happens to terrestrial organic matter in the ocean? *Organic Geochemistry*, *5–7*(27), 195–212. https://doi.org/10.1016/s0146-6380(97)00066-1

Henrichs, S. M., & Reeburgh, W. S. (1987). Anaerobic mineralization of marine sediment organic matter: Rates and the role of anaerobic processes in the oceanic carbon economy. *Geomicrobiology Journal*, *5*(3–4), 191–237. https://doi.org/10.1080/01490458709385971

Hulthe, G., Hulth, S., & Hall, P. O. (1998). Effect of oxygen on degradation rate of refractory and labile organic matter in continental margin sediments. *Geochimica et Cosmochimica Acta*, *62*(8), 1319–1328. https://doi.org/10.1016/s0016-7037(98)00044-1

Iversen, M. H. (2023). Carbon export in the ocean: A biologist's perspective. *Annual Review of Marine Science*, *15*(1), 357–381. https://doi.org/10.1146/annurev-marine-032122-035153

Jaccard, S. L., & Galbraith, E. D. (2012). Large climate-driven changes of oceanic oxygen concentrations during the last deglaciation. *Nature Geoscience*, *5*(2), 151–156. https://doi.org/10.1038/ngeo1352

Jahnke, R. A. (1996). The global ocean flux of particulate organic carbon: Areal distribution and magnitude. *Global Biogeochemical Cycles*, *1*(10), 71–88. https://doi.org/10.1029/95gb03525

Jahnke, R. A. (2010). Global synthesis. In K. Liu, L. Atkinson, R. Quiñones, & L. Talaue-McManus (Eds.), *Carbon and nutrient fluxes in continental margins*, *Global change—The IGBP series*. Springer. https://doi.org/10.1007/978-3-540-92735-8

Jin, X., Gruber, N., Dunne, J. P., Sarmiento, J. L., & Armstrong, R. A. (2006). Diagnosing the contribution of phytoplankton functional groups to the production and export of particulate organic carbon, $CaCO_3$, and opal from global nutrient and alkalinity distributions. *Global Biogeochemical Cycles*, *20*(2), GB2015. https://doi.org/10.1029/2005gb002532

Kallmeyer, J., Pockalny, R., Adhikari, R. R., Smith, D. C., & D'Hondt, S. (2012). Global distribution of microbial abundance and biomass in subseafloor sediment. *Proceedings of the National Academy of Sciences*, *109*(40), 16213–16216. https://doi.org/10.1073/pnas.1203849109

Keil, R. (2015). Hoard of fjord carbon. *Nature Geoscience*, *8*(6), 426–427. https://doi.org/10.1038/ngeo2433

Keil, R. G., Montluçon, D. B., Prahl, F. G., & Hedges, J. I. (1994). Sorptive preservation of labile organic matter in marine sediments. *Nature*, *370*(6490), 549–552. https://doi.org/10.1038/370549a0

Kristensen, E., & Holmer, M. (2001). Decomposition of plant materials in marine sediment exposed to different electron acceptors (O_2, NO_3^-, and SO_4^{2-}), with emphasis on substrate origin, degradation kinetics, and the role of bioturbation. *Geochimica et Cosmochimica Acta*, *65*(3), 419–433. https://doi.org/10.1016/s0016-7037(00)00532-9

Lamb, A. L., Wilson, G. P., & Leng, M. J. (2006). A review of coastal palaeoclimate and relative sea-level reconstructions using $\delta^{13}C$ and C/N ratios in organic material. *Earth-Science Reviews*, *75*(1–4), 29–57. https://doi.org/10.1016/j.earscirev.2005.10.003

La Rowe, D. E., Arndt, S., Bradley, J. A., Estes, E. R., Hoarfrost, A., Lang, S. Q., et al. (2020). The fate of organic carbon in marine sediments-New insights from recent data and analysis. *Earth-Science Reviews*, *204*, 103146. https://doi.org/10.1016/j.earscirev.2020.103146

Laruelle, G. G., Dürr, H. H., Lauerwald, R., Hartmann, J., Slomp, C. P., Goossens, N., & Regnier, P. A. G. (2013). Global multi-scale segmentation of continental and coastal waters from the watersheds to the continental margins. *Hydrology and Earth System Sciences*, *17*(5), 2029–2051. https://doi.org/10.5194/hess-17-2029-2013

Lee, T. R., Wood, W. T., & Phrampus, B. J. (2019). A machine learning (kNN) approach to predicting global seafloor total organic carbon. *Global Biogeochemical Cycles*, *33*(1), 37–46. https://doi.org/10.1029/2018gb005992

Levin, L. A., & Sibuet, M. (2012). Understanding continental margin biodiversity: A new imperative. *Annual Review of Marine Science*, *4*(1), 79–112. https://doi.org/10.1146/annurev-marine-120709-142714

Lutz, M., Dunbar, R., & Caldeira, K. (2002). Regional variability in the vertical flux of particulate organic carbon in the ocean interior. *Global Biogeochemical Cycles*, *16*(3), 11-1–11-18. https://doi.org/10.1029/2000gb001383

Martin, J. H., Knauer, G. A., Karl, D. M., & Broenkow, W. W. (1987). VERTEX: Carbon cycling in the northeast Pacific. *Deep-Sea Research, Part A: Oceanographic Research Papers*, *34*(2), 267–285. https://doi.org/10.1016/0198-0149(87)90086-0

Mayer, L. M., Rahaim, P. T., Guerin, W., Macko, S. A., Watling, L., & Anderson, F. E. (1985). Biological and granulometric controls on sedimentary organic matter of an intertidal mudflat. *Estuarine, Coastal and Shelf Science*, *20*(4), 491–503. https://doi.org/10.1016/0272-7714(85)90091-5

Mete, Ö., Subhas, A., Kim, H., Dunlea, A., Whitmore, L., Shiller, A., et al. (2023). Barium in seawater: Dissolved distribution, relationship to silicon, and barite saturation state determined using machine learning. *Earth System Science Data*, *15*(9), 4023–4045. https://doi.org/10.5194/essd-15-4023-2023

Middelburg, J. J. (2018). Reviews and syntheses: To the bottom of carbon processing at the seafloor. *Biogeosciences*, *15*(2), 413–427. https://doi.org/10.5194/bg-15-413-2018

Middelburg, J. J., Soetaert, K., & Herman, P. M. (1997). Empirical relationships for use in global diagenetic models. *Deep-Sea Research, Part I: Oceanographic Research Papers*, *2*(44), 327–344. https://doi.org/10.1016/s0967-0637(96)00101-x

Moore, O. W., Curti, L., Woulds, C., Bradley, J. A., Babakhani, P., Mills, B. J., et al. (2023). Long-term organic carbon preservation enhanced by iron and manganese. *Nature*, *621*(7978), 312–317. https://doi.org/10.1038/s41586-023-06325-9

Muller-Karger, F. E., Varela, R., Thunell, R., Luerssen, R., Hu, C., & Walsh, J. J. (2005). The importance of continental margins in the global carbon cycle. *Geophysical Research Letters*, *32*(1), L01602. https://doi.org/10.1029/2004gl021346

Nowicki, M., DeVries, T., & Siegel, D. A. (2022). Quantifying the carbon export and sequestration pathways of the ocean's biological carbon pump. *Global Biogeochemical Cycles*, *36*(3), e2021GB007083. https://doi.org/10.1029/2021gb007083

Orsi, W. D. (2018). Ecology and evolution of seafloor and subseafloor microbial communities. *Nature Reviews Microbiology*, *16*(11), 671–683. https://doi.org/10.1038/s41579-018-0046-8

Pedersen, T., & Calvert, S. E. (1990). Anoxia vs. productivity: What controls the formation of organic-carbon-rich sediments and sedimentary rocks?(1). *AAPG Bulletin*, *74*(4), 454–466. https://doi.org/10.1306/0c9b232b-1710-11d7-8645000102c1865d

Raven, M. R., Crotteau, M. A., Evans, N., Girard, Z. C., Martinez, A. M., Young, I., & Valentine, D. L. (2024). Biomass storage in anoxic marine basins: Initial estimates of geochemical impacts and CO_2 sequestration capacity. *AGU Advances*, *5*(1), e2023AV000950. https://doi.org/10.1029/2023av000950

Redfield, A. C. (1934). *On the proportions of organic derivatives in sea water and their relation to the composition of plankton* (Vol. 1). University Press of Liverpool.

Regnier, P., Resplandy, L., Najjar, R. G., & Ciais, P. (2022). The land-to-ocean loops of the global carbon cycle. *Nature*, *603*(7901), 401–410. https://doi.org/10.1038/s41586-021-04339-9

Rothman, D. H. (2024). Slow closure of Earth's carbon cycle. *Proceedings of the National Academy of Sciences*, *121*(4), e2310998121. https://doi.org/10.1073/pnas.2310998121

Røy, H., Kallmeyer, J., Adhikari, R. R., Pockalny, R., Jørgensen, B. B., & D'Hondt, S. (2012). Aerobic microbial respiration in 86-million-year-old deep-sea red clay. *Science*, *336*(6083), 922–925. https://doi.org/10.1126/science.1219424

Sarmiento & Gruber (2006). *Ocean biogeochemical dynamics*. Princeton University Press.

Smeaton, C., Cui, X., Bianchi, T. S., Cage, A. G., Howe, J. A., & Austin, W. E. N. (2021). The evolution of a coastal carbon store over the last millennium. *Quaternary Science Reviews*, *266*, 107081. https://doi.org/10.1016/j.quascirev.2021.107081

Smith, W. H. F., & Sandwell, D. T. (1997). Global sea floor topography from satellite altimetry and ship depth soundings. *Science*, *277*(5334), 1956–1962. https://doi.org/10.1126/science.277.5334.1956

Stanford, J. D., Hemingway, R., Rohling, E. J., Challenor, P. G., Medina-Elizalde, M., & Lester, A. J. (2011). Sea-level probability for the last deglaciation: A statistical analysis of far-field records. *Global and Planetary Change*, *79*(3–4), 193–203. https://doi.org/10.1016/j.gloplacha.2010.11.002

Steinberg, D. K., Van Mooy, B. A., Buesseler, K. O., Boyd, P. W., Kobari, T., & Karl, D. M. (2008). Bacterial vs. zooplankton control of sinking particle flux in the ocean's twilight zone. *Limnology & Oceanography*, *53*(4), 1327–1338. https://doi.org/10.4319/lo.2008.53.4.1327

Stumm, W., & Morgan, J. J. (1996). *Aquatic chemistry: Chemical equilibria and rates in natural waters* (3rd ed.). John Wiley & Sons.

Tegelaar, E. W., De Leeuw, J. W., Derenne, S., & Largeau, C. (1989). A reappraisal of kerogen formation. *Geochimica et Cosmochimica Acta*, *53*(11), 3103–3106. https://doi.org/10.1016/0016-7037(89)90191-9

Tegler, L. (2024). Data accompanying the manuscript "Distribution and drivers of organic carbon sedimentation along the continental margins" [Dataset]. *Mendeley Data, V2*. https://doi.org/10.17632/8fg4kthydv.2

Urey, H. C. (1952). *The planets: Their origin and development*. Yale University Press.

Volk, T., & Hoffert, M. I. (1985). The carbon cycle and atmospheric CO_2: Natural variations Archean to present. In *Geophysical Monograph Series* (pp. 99–110). https://doi.org/10.1029/gm032p0099

Walker, J. C. (1993). Biogeochemical cycles of carbon on a hierarchy of time scales. In *Biogeochemistry of global change: Radiatively active trace gases selected papers from the tenth international symposium on environmental biogeochemistry, San Francisco, August 19–24, 1991* (pp. 3–28). Springer US.

Westberry, T. K., Silsbe, G. M., & Behrenfeld, M. J. (2023). Gross and net primary production in the global ocean: An ocean color remote sensing perspective. *Earth-Science Reviews*, *237*, 104322. https://doi.org/10.1016/j.earscirev.2023.104322